

AD-A276 712

2

NASA Contractor Report 191547

ICASE Report No. 93-75

ICASE



THE RADIATED NOISE FROM ISOTROPIC TURBULENCE REVISITED

Geoffrey M. Lilley

DTIC
ELECTE
MAR 11 1994
S E D

NASA Contract No. NAS1-19480
December 1993

Institute for Computer Applications in Science and Engineering
NASA Langley Research Center
Hampton, Virginia 23681-0001

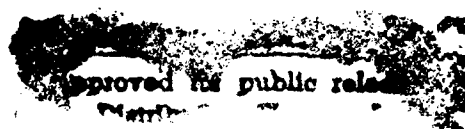
Operated by the Universities Space Research Association

94-07896



National Aeronautics and
Space Administration
Langley Research Center
Hampton, Virginia 23681-0001

94 3 10 032



**Best
Available
Copy**

ICASE Fluid Mechanics

Due to increasing research being conducted at ICASE in the field of fluid mechanics, future ICASE reports in this area of research will be printed with a green cover. Applied and numerical mathematics reports will have the familiar blue cover, while computer science reports will have yellow covers. In all other aspects the reports will remain the same; in particular, they will continue to be submitted to the appropriate journals or conferences for formal publication.

Accession For	
NTIS CRA&I	<input checked="" type="checkbox"/>
DTIC TAB	<input type="checkbox"/>
Unannounced	<input type="checkbox"/>
Justification	
By	
Distribution /	
Availability Codes	
Dist	Avail and/or Special
A-1	

THE RADIATED NOISE FROM ISOTROPIC TURBULENCE REVISITED.

Geoffrey M. Lilley*

Institute for Computer Applications in Science and Engineering
NASA Langley Research Center, Hampton, VA23665, USA.

Abstract

The noise radiated from isotropic turbulence at low Mach numbers and high Reynolds numbers, as derived by Proudman (1952), was the first application of Lighthill's *Theory of Aerodynamic Noise* to a complete flow field. The theory presented by Proudman involves the assumption of the neglect of retarded time differences and so replaces the second-order retarded-time and space covariance of Lighthill's stress tensor, T_{ij} , and in particular its second time derivative, by the equivalent simultaneous covariance. This assumption is a valid approximation in the derivation of the $\partial^2 T_{ij} / \partial t^2$ covariance at low Mach numbers, but is not justified when that covariance is reduced to the sum of products of the time derivatives of equivalent second-order velocity covariances as required when Gaussian statistics are assumed. The present paper removes these assumptions and finds that although the changes in the analysis are substantial, the change in the numerical result for the total acoustic power is small.

The present paper also considers an alternative analysis which does not neglect retarded times. It makes use of the Lighthill relationship, whereby the fourth-order T_{ij} retarded-time covariance is evaluated from the square of similar second-order covariance, which is assumed known. In this derivation no statistical assumptions are involved. This result, using distributions for the second-order space-time velocity squared covariance based on the Direct Numerical Simulation(DNS) results of both Sarkar and Hussaini(1993) and Dubois(1993), is compared with the re-evaluation of Proudman's original model. These results are then compared with the sound power derived from a phenomenological model based on simple approximations to the retarded-time/space covariance of T_{xx} . Finally the recent numerical solutions of Sarkar and Hussaini(1993) for the acoustic power are compared with the results obtained from the analytic solutions.

*This research was supported by the National Aeronautics and Space Administration under NASA Contract No. NAS1-19480 while the author was in residence at the Institute for Computer Applications in Science and Engineering (ICASE), NASA Langley Research Center, Hampton, VA 23681. Emeritus Professor, Department of Aeronautics and Astronautics, University of Southampton, U.K.

1.Introduction

Following the publication by Lighthill(1952) of 'The Theory of Aerodynamic Noise', Proudman(1952) considered the problem of its application to the generation of noise from isotropic turbulence. Batchelor(1951) had previously considered the pressure fluctuations in isotropic turbulence, and this proved to be an important first step in the consideration of the noise radiated from a finite volume of isotropic turbulence embedded in an otherwise infinite compressible medium at rest. Proudman discusses in great detail how Lighthill's Theory can be applied to this problem of isotropic turbulence. The theory requires information concerning the statistical properties of isotropic turbulence, including, in particular, the retarded-time and space covariance of the Lighthill stress tensor T_{ij} .

Proudman considers an infinite expanse of compressible fluid containing a finite region of turbulent motion, which generates sound radiating into the surrounding fluid, which is at rest, apart from the small motions characteristic of sound. Proudman assumes that the finite region of turbulent motion has been initially excited by some forcing function such that its initial characteristics are isotropic, and the turbulent Reynolds number, based on the velocity and length scale of the energy containing eddies, is very large. The turbulent kinetic energy then decays with time. Proudman discusses the contributions to the radiated sound from eddies of different length scales and reaches the conclusion that the generation of sound from the turbulence is mainly from two classes of eddies, those with scales in the dissipation range and those in the energy containing range. It is found that only the latter class of eddies make an appreciable contribution to the radiated sound at high Reynolds numbers. Proudman finds in general there are also two main contributions to the generated and thence radiated noise. The first arises from the decay of the turbulent kinetic energy while the second relates to its instantaneous generation. Proudman notes that in the initial period of decay, the effects of the retarded time between the source volume and the observer cannot be neglected even when the Mach number of the turbulence is small. The decay in the strengths of the equivalent acoustic sources is then so rapid that the intensity of sound outside the turbulence is dependent on the shape of the turbulent region and the turbulent energy decay law. Proudman suggests that the theory of aerodynamic noise, in the case of isotropic turbulence, is best applied to cases where the intensity of the turbulence is maintained constant in time during the processes of generation and radiation of the sound to the far-field. Also at low Mach numbers, the effects of the retarded time are small and can be neglected. Such conditions can only apply when the initial Reynolds number is very large. Thus the sound intensity in the far-field possesses a local time averaged value, and similarly for the total acoustic power. Accordingly the mean total acoustic power is a function of the time during the decay.

Proudman found to a good approximation that the total acoustic power radiated from this embedded finite region of turbulence contained within an infinite expanse of compressible fluid, is a function of the local time averaged kinetic energy of the turbulence per unit volume, K , and the time averaged rate of dissipation of the kinetic energy per unit volume, ϵ . We write $u \equiv \sqrt{\langle u^2 \rangle}$ as the characteristic velocity of the energy containing eddies. The corresponding characteristic length of the energy containing eddies we write as l , which is proportional to the integral scale of the turbulence, given below as L . In what follows, we assume l is of order L . In such an approximation, we can neglect the decay laws of the kinetic energy and the rate of dissipation of the kinetic energy and assume K and ϵ are functions independent of time during the calculation of the sound generation and its radiation. Here $\langle u^2 \rangle$ is $2K/3$, and during the decay we may put $\epsilon = 1.5u^3/L$. However,

we may consider, as does Proudman, the general case where noise is generated at any time in the decaying nonstationary turbulence provided the initial Reynolds number is sufficiently large. In isotropic turbulence when the flow is nearly incompressible, which is the case when the turbulent Mach number, $M = u/c_\infty$, is small and where c_∞ is the ambient speed of sound, we can write the simultaneous double-velocity correlation tensor between any two points A and B , distance r apart, in the turbulent flow, at a given time, t , as

$$Q_{ij}(r, t) = \langle u_i u_j \rangle = \langle u^2 \rangle \left[-\frac{1}{2r} f' r_i r_j + \left(f + \frac{r}{2} f' \right) \delta_{ij} \right], \quad (1.1)$$

where $f(r, t)$ is a scalar function of r , the distance between A and B , and dashes denote differentiation with respect to r . $\langle u^2 \rangle$ is the ensemble average of the longitudinal velocity components in the direction of A to B at either A or B . In isotropic turbulence Q_{ij} is *independent of position in the domain*. We write the integral length scale as

$$L(t) = \int_0^\infty f(r, t) dr. \quad (1.2)$$

Here $\langle u^2 \rangle$, $f(r, t)$, L , l , K , ϵ , and M are all functions of time during the decay of the turbulence from its given initial state. Similar results are obtained when the covariance is taken at different times at A and B . Q_{ij} and f are then functions of the time during the decay, the time separation between the times at A and B , and their space separation. Finally Proudman finds the total acoustic power as a function of u , L and f , only.

Proudman notes that the Lighthill theory takes full account of the propagation of sound through the turbulence, and variations of the sound speed through the turbulence as well as the back-reaction of the turbulence on the sound and the related, but very much weaker interaction, with the sound on the turbulence. Also at distances of many acoustic wavelengths from the turbulence, the radiation depends on the temporal differentiation of T_{ij} , provided the Mach number of the flow is small and the Reynolds number is large. Further at low Mach numbers the components of the turbulent intensity at a given frequency generate noise of the same frequency, such that the smallest acoustic wavelengths for which the acoustic energy is significantly different from zero must be very much larger than the characteristic length scales of the components of the turbulent energy (the larger eddies in the turbulence) generating the noise. In this case of low Mach number flows in the absence of a mean flow velocity, the proper matching conditions between the wave-numbers and frequencies in the turbulence and those in the far sound field are that the frequency of sound, ω , equals that in the turbulence, and the wave-number vector in the turbulence, k , is equal to $-(x/x)(\omega/c_\infty)$.

Proudman considers the case where the integral length scale of the turbulence, L , is very small compared with the typical dimension, D , of the turbulent domain. Proudman argues that the distance for the covariance to fall to zero must also be small compared with the dimensions of the turbulent region, D , in order that 'edge effects' from the boundaries to the turbulent domain will be relatively small. Within such a boundary layer, the turbulent intensity and vorticity fall to zero, and remains zero everywhere outside the region of turbulent flow. Within that boundary layer the turbulence is likely to be anisotropic and to have characteristics different from those in the central region of turbulent motion. Its thickness will be at least of order $3L$, and for the volume of the boundary region to be small compared with the total volume of turbulence, we must have

$L/D < O(1/100)$, say. (Such conditions are easy to specify in dealing with the problem analytically, but clearly present problems when considering the problem numerically.) Also the turbulence must not decay significantly in the time the sound takes to cross the turbulent region. Since the local eddy turnover time is $K/\epsilon = O(L/u)$, we find the Mach number of the turbulence, $M = u/c_\infty$, must satisfy the condition, $M \ll L/D \ll 1$, which is a very stringent condition indeed. Since the wavelength of the sound, λ_s , generated by the turbulence, at a frequency, ω , is given by $\lambda_s = 2\pi c_\infty/\omega$, the above condition is equivalent to L/λ_s being a very small quantity even at large values of the frequency, ω . We define the reference Strouhal number of the turbulence, $S_T = \Omega L/u$, which is $O(1)$, and where Ω is the reference frequency in the turbulence, is of order of the peak frequency in the turbulent energy spectrum. When $D\Omega/c_\infty \ll 2\pi$, the source is compact, and this is the case we are considering here. We emphasize these are the requirements for studying isotropic turbulence at low Mach numbers, or near incompressible flow, where, as discussed above, $M \ll 0.01$. The results obtained for the characteristics of the radiated noise, when applied to higher Mach numbers, need careful consideration.

Proudman finds at high Reynolds numbers that the acoustic power per unit volume of isotropic turbulence, $p_s \propto \rho_\infty \epsilon M^5$, and on substituting the relations for ϵ and M above, we find

$$p_s = \frac{\alpha \rho_\infty u^8}{c_\infty^5 L}, \quad (1.3)$$

where α , which we may call the Proudman constant, is a numerical constant. Its value is found by Proudman to depend on the shape of the longitudinal velocity scalar correlation function, $f(r/l)$. For $f(r/l) = \exp(-r^2/l^2)$, where $l = 2L/\sqrt{\pi}$, Proudman found the value $\alpha = 13.5$, whereas with Heisenberg's form for $f(r/L)$, as given by Batchelor(1953), $\alpha = 37.5$. During the decay, u and L vary with time. In self-preserving flow, where $K \propto t^{-1}$, and $L \propto t^{1/2}$, Proudman finds $p_s \propto t^{-9/2}$.

The theory presented below also considers the case of a very high initial turbulent Reynolds number. The results obtained by Proudman have been re-evaluated in the present paper and are compared with those obtained using the approach proposed by Lighthill(1992) whereby the fourth-order velocity covariance is derived from known values of the square of the similar second-order covariance. Results are also given using a phenomenological model for the $(T_{ij})_{tt}$ covariance. Finally the recent results of Sarkar and Hussaini(1993), based on Direct Numerical Simulations,(DNS), are compared with the analytic results. However these (DNS) results, and some further unpublished (DNS) results of Dubois(1993), have themselves guided to a very large extent, and in some cases confirmed, the assumptions made in the analytic theory of the acoustic noise generation from isotropic turbulence.

In the numerical work discussed below, the turbulence in a small unbounded region relative to the far-field observer as in Proudman's model, is assumed to have similar characteristics to those existing within any given box in an infinitely periodic domain. The turbulent flow in this given box is exposed to periodic boundary conditions unlike the boundary conditions which exist in the unbounded domain. The assumption is made that the noise generated within the given box can be considered in isolation of the remainder of the periodic domain and propagates its noise to the far-field observer as if the rest of the periodic domain were absent and replaced by fluid at rest of ambient density and speed of sound. The noise generated near the boundaries of the periodic box is not considered since the assumption is made that the turbulence in the vicinity of the boundaries meets the requirements specified above. Now numerous previous works using (DNS) have shown

that the overall characteristics of the turbulence, including the kinetic energy, K , and the dissipation rate, ϵ , in such a periodic box closely resemble those determined experimentally provided the integral scale, L , is small compared with the overall dimensions of the given box, D . However the Reynolds number of the turbulence is strictly limited in (DNS) to low Reynolds numbers, and thus the comparisons with the results of Proudman will be limited only to those cases where the integral scale, L , greatly exceeds the Taylor microscale, λ . We discuss below the problem that exists in the numerical simulations when the integral scale, L , is not sufficiently small compared with the computational box of side, D , to have no measurable effect on the longitudinal velocity correlation function, f . Such modifications to f are sufficient to change the characteristics of the computed acoustic power generated by the turbulence, and show, in aeroacoustics, that the demands on good spatial resolution in all length scales in (DNS) are more extreme, than in the corresponding calculations of the global statistical properties of the turbulence.

2. The Proudman model

Proudman finds, from Lighthill's Theory of Aerodynamic Noise, that the intensity of the radiated sound at a very large distance from an unbounded but finite domain of isotropic turbulence when the Mach number is small and the speed of sound in the turbulence is equal to its value in the ambient environment outside the turbulent flow, can be written

$$I(\mathbf{x}, t) = \frac{\rho_\infty}{16\pi^2 c_\infty^5 x^2} \iiint d\mathbf{y} \iiint d\mathbf{z} < \frac{\partial^2}{\partial \tau_A^2} u_x^2(\mathbf{y}, \tau_A) \frac{\partial^2}{\partial \tau_B^2} u_x^2(\mathbf{z}, \tau_B) >, \quad (2.1)$$

where u_x is the turbulent velocity component in the direction between the source and the observer.

Here the component of the Lighthill stress tensor, T_{ij} , in the direction from source to observer, has been assumed equal to $\rho_\infty(u_x^2 - \langle u_x^2 \rangle)$, and in the above integral the fluctuations of u_x^2 about its local mean value during the decay are implied. ρ_∞ and c_∞ are the constant density and speed of sound throughout the turbulent flow and in the radiation domain outside it. The retarded times at A and B are respectively, $\tau_A = t - |\mathbf{x} - \mathbf{y}|/c_\infty$, and $\tau_B = t - |\mathbf{x} - \mathbf{z}|/c_\infty$. Proudman reduces the second-order space time covariance of T_{ij} to a series of second order velocity covariances on the assumption that in isotropic turbulence the velocity at two separated points in space has a normal joint probability distribution. Proudman also invokes the Navier-Stokes equations to convert pressure covariances into functions of the velocity covariances as well as reducing the time gradient of the velocity covariances to spatial gradients of the two-point longitudinal velocity correlation function, $f(r, t)$. Finally the T_{ij} covariance is evaluated for two different forms of the self-preserving function, $f(r/L(t))$, where the integral length scale, L , is a function of time, and this in turn determines the value of the Proudman constant, α , in Equation(1.3) above.

In Proudman's high Reynolds number model it is assumed that for isotropic turbulence in near incompressible flow the effects of retarded time in the evaluation of the two-point covariance of $\partial^2 T_{ij}/\partial t^2$ can be neglected. This approximation is used throughout the analysis and, in particular, with the reduction of the above two-point covariance into the sum of covariances of the time derivatives of the velocity components. But a time derivative at a point A inside the turbulence differs from the time derivative at a point B and even though the differences are small they are not negligible as can be shown in the following analysis.

We find that the covariance of $(T_{ij})_{tt}$ between the two points A and B at times t_A and t_B respectively, where the aligned velocity components are, writing u for u_x , $u = u_A$ and $u' = u_B$ respectively, and the density is assumed constant and equal to unity, is given by the scalar function, U ,

$$U = \langle \frac{\partial^2}{\partial t_A^2} (u_A^2 - \langle u^2 \rangle) \frac{\partial^2}{\partial t_B^2} (u_B^2 - \langle u^2 \rangle) \rangle, \quad (2.2)$$

since in isotropic turbulence $\langle u^2 \rangle = \langle u_A^2 \rangle = \langle u_B^2 \rangle$. Now covariances in isotropic turbulence are normally evaluated in terms of the velocity components, u_i , and their derivatives at A and B , whereas T_{ij} involves the quadratic components, $u_i u_j$. Thus we need to expand the derivatives in equation (2.2). Using the notation $(\partial u / \partial t_A)^2$ equals $u_{t_A}^2$, and similarly with respect to the other terms, and with $u_A = u$, and $u_B = u'$, it follows that:

$$\begin{aligned} U = & 4(\langle (u_{t_A})^2 (u'_{t_B})^2 \rangle - \langle (u_{t_A})^2 \rangle \langle (u'_{t_B})^2 \rangle + \langle (u_{t_A})^2 u'_{t_B t_B} \rangle - \\ & \langle (u_{t_A})^2 \rangle \langle u'_{t_B t_B} \rangle + \langle u u_{t_A t_A} (u'_{t_B})^2 \rangle - \langle u u_{t_A t_A} \rangle \langle (u'_{t_B})^2 \rangle + \\ & \langle u u_{t_A t_A} u'_{t_B t_B} \rangle - \langle u u_{t_A t_A} \rangle \langle u'_{t_B t_B} \rangle), \end{aligned} \quad (2.3)$$

which involves a set of both fourth and second-order covariances. Proudman used a similar notation, except $t = t_A = t_B$ was introduced throughout. Equations (2.2) and (2.3) are the starting points for both the analysis in this section and in the work of Proudman(1952).

Following the work of Batchelor(1951) and Proudman(1952) we assume the joint probability distribution between the velocities at A and B is normal and so the fourth-order covariances may be replaced with second-order covariances in pq and $p'q'$ using the Millionshtchikov relations :

$$\langle (pq)_A (p'q')_B \rangle = \langle pq \rangle \langle p'q' \rangle + \langle pp' \rangle \langle qq' \rangle + \langle pq' \rangle \langle qp' \rangle. \quad (2.4)$$

Thus we find that:

$$\begin{aligned} U = & 8 \langle u_{t_A} u'_{t_B} \rangle^2 + 4 \langle u u' \rangle \langle u_{t_A t_A} u'_{t_B t_B} \rangle + 4 \langle u u'_{t_B t_B} \rangle \langle u' u_{t_A t_A} \rangle + \\ & 8 \langle u u'_{t_B} \rangle \langle u_{t_A t_A} u'_{t_B} \rangle + 8 \langle u_{t_A} u' \rangle \langle u_{t_A} u'_{t_B t_B} \rangle. \end{aligned} \quad (2.5)$$

This equation differs from that given by Proudman(1952) for reasons that will be discussed below, in this section, and also in Appendix 3. It involves only products of two-point second-order velocity covariances. In order to clarify the further reduction of this formula we will use a different but more compact notation.

Let A and B be the points with coordinates y and z respectively, with source times t_A and t_B respectively. With this notation we find:

$$U = 8S_{AB}^2 + 4R_{AB}T_{AB} + 4V_1 + 8(V_2 + V_3) \quad (2.6)$$

where, since u_A is a constant when differentiating with respect to t_B and u_B is a constant when differentiating with respect to t_A ,

$$R_{AB} = \langle u_A u_B \rangle. \quad (2.7a)$$

$$S_{AB} = \langle \frac{\partial u_A}{\partial t_A} \frac{\partial u_B}{\partial t_B} \rangle = \frac{\partial^2 R_{AB}}{\partial t_A \partial t_B}. \quad (2.7b)$$

$$T_{AB} = \langle \frac{\partial^2 u_A}{\partial t_A^2} \frac{\partial^2 u_B}{\partial t_B^2} \rangle = \frac{\partial^4 R_{AB}}{\partial t_A^2 \partial t_B^2}. \quad (2.7c)$$

$$V_1 = \langle u_A \frac{\partial^2 u_B}{\partial t_B^2} \rangle = \langle u_B \frac{\partial^2 u_A}{\partial t_A^2} \rangle = \frac{\partial^2 R_{AB}}{\partial t_A^2} \frac{\partial^2 R_{AB}}{\partial t_B^2}. \quad (2.7d)$$

$$V_2 = \langle u_A \frac{\partial u_B}{\partial t_B} \rangle = \langle \frac{\partial u_B}{\partial t_B} \frac{\partial^2 u_A}{\partial t_A^2} \rangle = \frac{\partial R_{AB}}{\partial t_B} \frac{\partial^3 R_{AB}}{\partial t_B \partial t_A^2}. \quad (2.7e)$$

$$V_3 = \langle u_B \frac{\partial u_A}{\partial t_A} \rangle = \langle \frac{\partial u_A}{\partial t_A} \frac{\partial^2 u_B}{\partial t_B^2} \rangle = \frac{\partial R_{AB}}{\partial t_A} \frac{\partial^3 R_{AB}}{\partial t_A \partial t_B^2}. \quad (2.7f)$$

In the case of stationary turbulent flow R_{AB} is dependent on $\tau = t_B - t_A$ only and then

$$U = 12 \left(\frac{\partial^2 R_{AB}}{\partial \tau^2} \right)^2 + 4 R_{AB} \frac{\partial^4 R_{AB}}{\partial \tau^4} + 16 \left(\frac{\partial R_{AB}}{\partial \tau} \frac{\partial^3 R_{AB}}{\partial \tau^3} \right). \quad (2.8)$$

The corresponding result from Proudman's analysis, as shown in Appendix 3, is

$$U = 9 \left(\frac{\partial^2 R_{AB}}{\partial t^2} \right)^2 + 4 R_{AB} \frac{\partial^4 R_{AB}}{\partial t^4} + 4 \left(\frac{\partial R_{AB}}{\partial t} \frac{\partial^3 R_{AB}}{\partial t^3} \right), \quad (2.9)$$

where although the same terms arise the numerical coefficients are different from those in Equation (2.8). The difference between the two analyses lies simply in that Proudman has put $t_A = t_B = t$ at the start of the analysis, whereas in our analysis we have introduced this approximation at the end. To that extent both treatments are approximate, but we contend that our present analysis is more justifiable than the earlier approximation introduced by Proudman. The differences involved are presented and discussed at greater length in Appendix 3. In Proudman's work t is the source time and includes both the effects of the decay time and the temporal fluctuations between A and B in deriving Equation(2.9). If, like Proudman(1952), we neglect retarded times, then $t = t_A = t_B$, and Equation(2.8) remains unchanged except τ must be replaced by t . The general expressions for U , as given in Appendix 3, show greater differences. With the general expression for U we can find the separate effects of time during the decay and time separation effects between t_A and t_B .

If we now evaluate the value of the Proudman constant, α , following the method used by Proudman(1952), but using Equation(2.8) in place of Equation(2.9) we find, as given in Appendix 3, for the case when the two-point longitudinal velocity correlation function $f(r/L) = \exp(-\pi r^2/4L^2)$, that $\alpha = 10.96$, compared with Proudman's result $\alpha = 13.5$, for this same correlation function. (In a recent revised calculation of α , based exactly on the same formula used by Proudman, we find $\alpha = 12.5$.)

3. A Simplified Model.

An alternative, and simpler form, can be obtained for the T_{ij} covariance and its second time derivative when the turbulence is pseudo-stationary. In such a case we can write the intensity of the radiated sound as follows:

$$I(\mathbf{x}, t) = \frac{\rho_{\infty}}{16\pi^2 c_{\infty}^5 x^2} \iiint d\mathbf{y} \iiint d\mathbf{r} \frac{\partial^4}{\partial \tau^4} P_{xx,xx}(\mathbf{y}, \mathbf{r}, \tau), \quad (3.1)$$

and from this we can find the total radiated acoustic power output per unit volume of turbulence.

Here $P_{xx,xx}$ is the space-time covariance of $(T_{xx} - \langle T_{xx} \rangle)$, with ρ replaced by its approximately constant value ρ_{∞} , and which, in isotropic turbulence, is independent of the position \mathbf{y} inside the flow. To our approximation, as discussed above, the T_{xx} covariance is reduced to that of $(u_x^2 - \langle u_x^2 \rangle)$. We assume that $P_{xx,xx}$, beyond certain values of $|\mathbf{r}|$ and τ , is a decreasing function of the separation distance r and the retarded time separation τ , and falls to zero in a distance small compared with the dimensions of the assumed large turbulence volume. In the general case of decaying isotropic turbulence, it is also a function of the time, t , during the decay period, since $\langle u^2 \rangle$, and the integral length scale of the turbulence, L , must both depend on t . We assume that a physically possible form for $P_{xx,xx}$ at sufficiently high Reynolds numbers is the self-preserving function

$$P_{xx,xx} = u^4 \Phi(r/l) \Psi(\Omega\tau), \quad (3.2)$$

with the non-dimensional space correlation function, $\Phi(r/l)$, and the non-dimensional retarded time correlation function, $\Psi(\Omega\tau)$ being chosen so that the dominant portions of the spectra of the velocity fluctuations are adequately resolved. Here u , l , and Ω are respectively reference values of the turbulent velocity, the turbulent length scale, and turbulent frequency, and, in general are all functions of time during the period of decay. In stationary turbulence they are constants. Currently there is little experimental evidence to provide a guide for a suitable correlation function in both space and time, due to the technical difficulties in measuring the fourth-order velocity covariance and both the fluctuating pressures and densities involved in T_{ij} in any flow field, and in particular in isotropic turbulence. (However guidance as to appropriate functional forms for Φ and Ψ can be obtained by considering the similar functions relating to the two-point velocity covariances.) We do not suggest that the self-preserving relation given in Equation(3.2), using a separation of variables, is the most general or only possible form for $P_{xx,xx}$ even in the case, as considered here, when the turbulence is assumed self-preserving.

The introduction of a self-preserving and separation of variables form for $P_{xx,xx}$ implies that it would be most applicable in a domain where one type of flow prevails. This would be possible in either of the limits of very low or very high turbulent Reynolds numbers. Here we prefer to consider only the case of very high turbulent Reynolds numbers. We therefore assume that this type of flow holds throughout the complete spatial domain during the total decay of the isotropic turbulence, where the energy containing length scales of order, l , are very large compared with the Taylor microscale eddies of order, λ . The decomposition of the far-field sound intensity into its spectral components and the corresponding decomposition of the equivalent acoustic source function, $P_{xx,xx}$, into its wave-number components, \mathbf{k} , and frequency, ω , suggests an independence of wave-number and frequency and correspondingly an independence of space and time in the characteristics of $P_{xx,xx}$. An independence principle of the space and time characteristics of $P_{xx,xx}$

corresponds to the approximation involving a separation of variables as given by Equation(3.2). Of course such independence is artificial in the acoustics problem since we have a coupling condition between frequency and wave-number for sound waves in the domain outside the turbulence, and a corresponding matching relationship exists between the wave-number and frequency components in the four-dimensional Fourier transform of $P_{xx,xx}$, which we write in the form, $P(\mathbf{k}, \omega)$, as given in Appendix(4) below. Correspondingly we see that the space-time covariance is connected through the far-field retarded time relation $t^* = \tau + \mathbf{k} \cdot \mathbf{r} / \omega$, where t^* is the autocorrelation time separation at the observer. Thus, by reference to Equation(3.1), we see that for each value of the space separation we need the fourth time derivative of $P_{xx,xx}$ evaluated at $\tau = t^* - \mathbf{k} \cdot \mathbf{r} / \omega$. The contribution to the far-field intensity, and hence the total acoustic power, involves the volume integration of the fourth-order covariance, $\partial^4 P_{xx,xx} / \partial \tau^4$ over all values of \mathbf{r} . Since the elemental volume is, $r^2 \sin \theta d\theta d\phi dr$, we find that the integrand peaks at a value of r distant from $r = 0$. At $r = 0$ its value is zero. A simple example shows that near the peak in the integrand we have values of r of order the length scale of the energy containing eddies, and the fourth time derivative, taken at this value of r at $\tau = t^* - \mathbf{k} \cdot \mathbf{r} / \omega$, will also be related to times involving the energy containing eddies. Thus from an inspection of the four-dimensional mapping of $P_{xx,xx}$ in the space-time domain we find its dominant contribution to the integrand in Equation(3.1) centres on a peak at a distance, r , of order l , and a time, τ , of order $1/\Omega = l/u$ with respect to the origin. Hence in the modelling of this dominant contribution to the total acoustic power we find it is possible, as suggested above, to reduce the space-time covariance to the product of the separate space and time covariances. If for any reason the integrand in Equation(3.1) had peaked near $r = 0$, such a separation of variables would have been physically less acceptable, but then the space-time interaction would have involved a major contribution from small scale turbulence in that domain. At high Reynolds numbers in unbounded domains such as are being considered here, the dominant contribution to the generation of sound from a turbulent flow arises, as found by Lighthill(1952), from the dynamics of the highly energetic parts of the turbulent motion, namely the energy containing scales.

In the region of final decay in isotropic turbulence, where inertial effects are small and can be neglected, it is known, for this domain of low turbulent Reynolds numbers, that the simultaneous two-point longitudinal velocity correlation function is $f(r, t) = \exp(-r^2/8\nu t)$, which in self-preserving flow becomes, $f(r, t) = \exp(-r^2/2\lambda^2)$, where λ , the Taylor microscale, is a function of time. At earlier times in the decay, $f(r/L) = \exp(-r/L)$, except at small and very large spatial separations, where $f(r/L) = \exp(-c(r/L)^2)$, with c a constant, and is found to approximate to the function as measured experimentally at higher turbulent Reynolds numbers. We also note that in the (DNS) results discussed in Section(5) the initial turbulent energy spectrum is given the distribution $k^4 \exp(-2k^2/k_m^2)$ which corresponds to $f(r/L) = \exp(-\pi/4(r/L)^2)$. k_m is the wave-number at the peak in the energy spectrum. One of the forms used by Proudman(1952) for $f(r/L)$ was also equal to this latter function. Thus, arising from these observations, and noting $P_{xx,xx}$ involves the velocity squared covariance, we suggest that a possible form for the space covariance, $\Phi(r/l)$, is $\exp(-2(r/l)^2)$. (A better choice at high Reynolds numbers is possibly $\exp(-r/l)$ but this has the disadvantage of not having finite curvature at $r = 0$, which is a necessary condition at all Reynolds numbers since the dissipation range of wave-numbers and frequencies is finite. On balance the choice of a Gaussian distribution function appears to be a better choice.) A first choice for the temporal covariance $\Psi(\Omega\tau)$ is made on similar assumptions and we put $\Psi(\Omega\tau) = \exp(-\pi\Omega^2\tau^2/2)$. This function is however a very poor approximation to the temporal covariance at times greater than zero where the corresponding turbulent frequency spectrum has a much richer population in the higher frequencies arising from non-linear interactions. The spectrum corresponding to $\Psi(\Omega\tau) = \exp(-\pi\Omega^2\tau^2/2)$ does not capture the full amplitude of the higher frequencies, and the

(DNS) simulations discussed below, show the differences between the assumed and calculated spectra. This form of $\Psi(\Omega\tau)$ does have the merit, however, that it captures the characteristics of the lower frequencies and near the peak frequencies in the spectrum.

Since $dK/dt = -\epsilon$ holds throughout the decay and we assume the conditions for self preserving flow remain throughout, we find K is proportional to t^{-1} . This, together with two important length scales in the turbulence, defines the dynamic behaviour of the turbulence during the decay. These length scales are l , the energy containing scale, and λ , the Taylor microscale, which is defined from the dissipation function, ϵ , with

$$\epsilon = 15\nu \frac{u^2}{\lambda^2}, \quad (3.3)$$

where ν is the kinematic viscosity. λ is also defined in isotropic turbulence as the radius of curvature of the scalar longitudinal velocity correlation function, $f(r, t)$, at the origin, or

$$\left(\frac{\partial^2}{\partial r^2} f(r, t) \right)_{r=0} = -\frac{1}{\lambda^2}. \quad (3.4)$$

Thus even at high Reynolds numbers the longitudinal velocity correlation function, $f(r)$, near $r = 0$, is a function of Reynolds number, since its curvature there depends on λ , and λ itself is a function of Reynolds number. Away from the origin $f(r)$ is a function of r/L where the integral length scale is a measure of the scale of the energy containing eddies which are responsible for the bulk of the noise generated from the turbulence at high enough Reynolds numbers. The time covariance of the velocity, for any given spatial separation, has a smaller curvature near the origin, $\tau \rightarrow 0$, than that of the corresponding spatial correlation as $r \rightarrow 0$, since at high Reynolds numbers this covariance has properties related to that of the pressure covariance, and hence depends on all scales of turbulence. In this initial region, it can be shown that both λ and L increase with time proportional to $t^{1/2}$. In the final period of decay, which is viscous dominated, λ continues to increase proportional to $t^{1/2}$. However in this region we find L decreases with time proportional to $t^{-1/4}$. In the initial region, if the flow is self-preserving, we can use either λ or L as the characteristic length in defining the similarity forms of the spatial correlation function, since λ is proportional to L . However since in the problem of sound radiation from isotropic turbulence it appears, at high values of the Reynolds number and in the main period of decay, that the bulk of the noise is found to originate from scales of turbulence only slightly smaller than those containing most of the energy, we prefer to use l as the characteristic length scale in the turbulence throughout the decay. In the recent study of Speziale and Bernard(1992), it is shown that the conditions for decaying self-preserving isotropic turbulence are that K should be proportional to t^{-1} and $R_\lambda = u\lambda/\nu$ is equal to a constant throughout the decay, with the so-called asymptotic final period of decay, in which K falls as $t^{-5/2}$, only being reached as $t \rightarrow \infty$. Thus in a domain of self-preserving isotropic turbulence we see that $R_L = uL/\nu$ also remains constant throughout the entire region of decay, with u decreasing as $t^{-1/2}$ and both λ and L increasing as $t^{1/2}$. The initial conditions must be such that the flow field is initially isotropic at a sufficiently high Reynolds number, R_L . The value of the constant asymptotic Reynolds number, R_λ , depends critically on its initial joint probability distribution and in particular its velocity derivative flatness and skewness. In most experiments on the decay of isotropic turbulence the turbulence is not fully self-preserving and K falls close to t^{-s} , where $s = 1.24$ to 1.34 rather than the t^{-1} as found in self-preserving isotropic turbulence. This is

also the case in the (DNS) results as will be shown below. For further details on the characteristics of self-preserving isotropic turbulence refer to Speziale and Bernard(1992). The main characteristics of isotropic turbulence are listed in Appendix 1.

With these functions Φ , Ψ and f we find there are two parameters, l or L , and Ω , which we relate respectively to the length scale and frequency of the energy containing eddies. Since we have already introduced u as the characteristic velocity of the isotropic turbulence, which we have put equal to the root mean square velocity in any direction, it follows, as described above, that we may write, $S_T = \Omega L/u$ as the Strouhal number of the turbulence which we assume is independent of space and time. In general we might expect S_T to have a value of order unity. In the stationary case, where K remains independent of time, the dominant time scale in the turbulence is $1/\Omega$, corresponding to that of the fluctuations of the energy containing scales. This time scale, which we may refer to as an integral time scale, is also of order L/u , giving, as stated above, a value for S_T of order unity. In this case u , L and Ω are all independent of time. When the turbulence is decaying there are now two time scales, $1/\Omega$ and that associated with the time scale of the decay, which we call, t_D , and is the time for the initial values of K_0 and ϵ_0 to fall to their vanishingly small values at the end of the decay. Such a time t_D is clearly of order K_0/ϵ_0 , and we put $t_D = K_0/\epsilon_0$, say. If then we write $\Omega_0 = 1/t_D$ we find $\Omega_0 = \omega_0/\sqrt{3/2 R_{L_0}}$, where ω_0 is the initial rms vorticity, and R_{L_0} is the initial Reynolds number. Thus when R_{L_0} is very large Ω_0 is very small, and $\Omega_0 < u_0/L_0$. Thus we find t_D is a long time scale. (At $t = 0$ we find that $\epsilon_0 \neq 3/2 u_0^3/L_0$, its equilibrium value.) Hence at all times beyond the initialization regime, where the turbulence is readjusting itself from its initially imposed conditions at time $t = 0$, we find the time scale of the dominant fluctuations in the turbulence is the short time scale, $t_s = 1/\Omega = L/u$, with $t_s \ll t_D$. However for small values of the initial Reynolds number, R_{L_0} , we fail to obtain a time during the decay when a large separation exists between t_s and t_D , moreover Ω and Ω_0 are of similar orders of magnitude. At high Reynolds numbers $\Omega \gg \Omega_0$. In this section we assume the Reynolds number is sufficiently high so that in both the stationary and non-stationary cases $\Omega \gg \Omega_0$, except during the short initial period following the commencement of the decay. Then, as stated above the integral time scale t_s is of order L/u and the turbulent Strouhal number, $S_T = 1$.

However in the (DNS) simulations of Sarkar et al(1993), which are discussed in Section(5) below, the Reynolds number is not large and Ω and Ω_0 are of similar orders of magnitude. It has thus proved difficult to extract, from the databank of these simulations, definitive values for Ω . However in these results we find to a good approximation, at about half the initial eddy turnover time, that a good value for the turbulent Strouhal number is $S_T = 1$. In the case of the (DNS) simulations by Dubois(1993) using forced turbulence, the values of K and ϵ remain almost constant for a large part of the decay and for all practical purposes the turbulence may be regarded as stationary. But in that case also it has proved difficult to find values of the integral time scale, and hence Ω , since at large separation distances and times the T_{ij} covariance is adversely affected by the forcing amplitude, and therefore produces a contamination on both the integral length and time scales. These results are discussed in detail in Section(5) below.

For the reasons discussed above the space-time correlation function may be written:

$$P_{xx,xx} = u^4 \exp \left(-\frac{\pi}{2} \left(\frac{r^2}{L^2} + \Omega^2 \tau^2 \right) \right), \quad (3.5)$$

with its four-dimensional wave-number/frequency spectrum function:

$$P(\mathbf{k}, \omega) = \frac{1}{4\pi^4} \frac{u^7 S_T^3}{\Omega^4} \exp\left(-\frac{\omega^2}{2\pi\Omega^2} C\right), \quad (3.6)$$

and with the acoustic power spectral density, as found in Appendix 4,

$$p_s(\omega) = 2\pi^2 \frac{\rho_\infty}{c_\infty^5} \omega^4 P(\mathbf{k}, \omega), \quad (3.7)$$

where $C = 1 + S_T^2 u^2 / c_\infty^2$, and showing a peak in the acoustic power spectrum at a frequency $\omega_m = \sqrt{8}\Omega$. At low Mach numbers, where u/c_∞ is small, C has a value of near unity. With this wave-number/frequency spectrum function the total radiated acoustic power per unit volume of turbulence is:

$$\begin{aligned} p_s &= \frac{\rho_\infty u^3 L^4}{\pi^2 c_\infty^5 S_T} \int_0^\infty \omega^4 \exp\left(-\frac{\omega^2}{2\pi\Omega^2} C\right) d\omega \\ &= \frac{3\pi\rho_\infty S_T^4 u^8}{\sqrt{2} L c_\infty^5 C^{5/2}}. \end{aligned} \quad (3.8)$$

Throughout we have assumed that the characteristic length scale of the of the T_{xx} covariance is approximately equal to the scale of the energy containing eddies, L .

This result makes no approximations with respect to the retarded time differences, but its value depends critically on the distributions chosen for Φ and Ψ in $P_{xx,xx}$, and the value of the reference turbulent Strouhal number, S_T . If S_T is given the value 1.25 then the value of the Proudman constant, α , as defined in Equation(1.3), is equal to 16.26, but if $S_T = 1$ then $\alpha = 6.66$. The results from Proudman's model give numerically similar results with α in the range 13.5 to 37.5 depending on the chosen form for $f(r/L)$. In fact Proudman refers to values of α as order of magnitude values only, since unless $f(r/L)$ is known for the given flow any inaccuracy in $f(r/L)$ is also reflected in the value of α . Our experience is that small changes in $f(r/L)$ generate large changes in the Proudman constant, α . We found in Section 2, for the case of stationary flow, when $f(r/L) = \exp(-\pi r^2/4L^2)$,

$$p_s = \frac{10.96\rho_\infty u^8}{L c_\infty^5}, \quad (3.10)$$

or $\alpha = 10.96$.

If we had assumed space and time covariances were proportional to exponential functions we would have found that the noise generated would have over-emphasized the contributions from the eddies of length scales of the order of the Taylor microscale. The resulting noise would have been of very high frequency. But as stated above, it is our contention, that the small eddies controlling the space-time covariance near the origin of the space and time separations, do not control the dominant regions of the space-time covariance contributing most to the generation of noise at high turbulent Reynolds numbers. This region is displaced from the origin and is centered more towards those eddies containing most of the energy in the turbulence. Thus in choosing empirical functions for the non-dimensional correlation functions in space and time we concentrate only on functions which provide an adequate representation of the space-time covariance at distances of order L and times of order $1/\Omega$ and which vanish at large separation distances and times. But most important

of all we choose a space-time covariance which is a function of τ/L and $\Omega\tau$ only, with L and Ω constant in a stationary turbulent flow, and functions of time in non-stationary turbulent flows, and which are independent of the flow Reynolds number above high enough Reynolds numbers. In non-stationary self-preserving flows both L/u and $1/\Omega$ increase linearly with time giving $S_T = \text{a constant}$, which we put equal to unity. Definitive values for S_T have yet to be determined. Our final values for the Proudman constant, α , are independent of Reynolds number but remain sensitive to the turbulent Strouhal number, S_T , which is a parameter which must be determined from experiment or from further (DNS) or (LES) simulations. It seems, however, unlikely that we will be able to construct an experiment from which S_T will be found experimentally. A guide to the selection of results from the numerical simulations in respect of the Reynolds numbers of the Taylor microscale, R_λ , and the integral scales, R_L , can be found in Table 3, along with the ratios of the various turbulent length scales and turbulent frequencies. The decay laws for self-preserving isotropic decaying turbulence are presented, as stated above, in Appendix 1 and listed in Tables 1 and 2.

If we model the acoustic spectrum as found in the (DNS) results of Sarkar et al(1993) we find, as shown in Figure(1), that the measured spectrum increases approximately as ω^2 in the low frequencies and falls as ω^{-2} in the high frequencies before falling rapidly in the dissipation range. However due to the dependence of the temporal covariance on $\partial^4/\partial\tau^4$ the spectrum must increase as ω^4 at very low frequencies. A simple analytic expression, which satisfies this low frequency condition and fits the measured results up to the high frequency ‘dissipation cut-off’, is $\omega^4/(1 + \omega^2/4\Omega^2)^3$, corresponding to the temporal covariance $(1 + 2\Omega\tau + 4/3\Omega^2\tau^2)\exp(-2\Omega\tau)$. The comparison between the (DNS) results and the model expression for the acoustic spectrum is shown in Figure(2) and the corresponding temporal part of the T_{xx} covariance is shown in Figure(3). Figure(3) also shows the comparison with the DNS results of Dubois(1993). These are discussed in Section(5) below. Figure(4) shows the comparison between the (DNS) spectrum and that found using the Gaussian approximation for the temporal covariance as given in Figure(5). Although the Gaussian approximation fits the peak in the spectrum it under-predicts at both the low and high frequencies. A comparison between Figures(2) and (4) shows the improvement in agreement with the DNS results using the $1/\omega^2$ law at frequencies greater than the peak frequency. The corresponding changes in the temporal part of the T_{xx} covariance are shown in Figures(3) and (5), for the $1/\omega^2$ and the Gaussian laws respectively. A much greater difference can be seen in the fourth time derivatives of these covariances as shown in Figures(6) and (7) for the Gaussian and $1/\omega^2$ laws respectively. In both cases, and indeed for all covariances, the integral over all time separations is zero. Again we see large differences in their behaviour near the origin, the Gaussian being well-rounded whereas the $1/\omega^2$ is very spikey. The total acoustic power using the Gaussian time covariance was found above from Equation(3.9), and resulted in a Proudman constant, $\alpha = 5.32$, when the turbulent Strouhal number, $S_T = 1.0$. For the $1/\omega^2$ spectrum function, with no truncation at high frequencies in the dissipation range, the value of $\alpha = 6.26$ for a Strouhal Number, $S_T = 1.0$, and $\alpha = 15.29$ for a Strouhal number, $S_T = 1.25$. The importance of the turbulent Strouhal number in determining the value of the Proudman constant is thus obvious and hence the results obtained from this section must be regarded as very approximate, except where independent data on the values of the turbulent Strouhal number, the longitudinal velocity correlation function and the acoustic spectrum are available for calibration. The detailed discussion of the (DNS) results is given in Section(5) below, where further comparison is given between the results obtained in this section together with the results found in the next section.

4. The Direct Evaluation of the Total Acoustic Power using the Lighthill Relationship.

Proudman finds, from Lighthill's *Theory of Aerodynamic Noise*(1952), that the intensity of the radiated sound at a very large distance from an unbounded but finite domain of isotropic turbulence when the Mach number is small and the speed of sound in the turbulence is equal to its value in the ambient environment outside the turbulent flow, can be written

$$I(\mathbf{x}, t) = \frac{\rho_\infty}{16\pi^2 c_\infty^5 x^2} \iiint d\mathbf{y} \iiint d\mathbf{z} < \frac{\partial^2}{\partial \tau_A^2} u_x^2(\mathbf{y}, \tau_A) \frac{\partial^2}{\partial \tau_B^2} u_x^2(\mathbf{z}, \tau_B) >, \quad (4.1)$$

where u_x is the instantaneous turbulent velocity component in the direction between the source and the observer. Here the component of the Lighthill stress tensor, T_{ij} , in the direction from source to observer has been assumed equal to $\rho_\infty(u_x^2 - \langle u_x^2 \rangle)$, and in the above integral the fluctuations of u_x^2 about its local mean value during the decay are implied. ρ_∞ and c_∞ are the constant density and speed of sound throughout the turbulent flow and in the radiation domain outside it.¹ The retarded times at A and B are respectively, $\tau_A = t - |\mathbf{x} - \mathbf{y}|/c_\infty$, and $\tau_B = t - |\mathbf{x} - \mathbf{z}|/c_\infty$. We base our prediction on the direct evaluation of the fourth-order covariance and not on its reduction to the sum of products of corresponding second order covariances based on Gaussian statistics, as assumed in Proudman's work. In the radiated sound field, the total sound power per unit volume is given by

$$p_s = \frac{\rho_\infty}{4\pi c_\infty^5} \iiint U d\mathbf{r}, \quad (4.2)$$

where the equivalent acoustic source function, U , is given by

$$U = < \frac{\partial^2}{\partial \tau_A^2} (u_A^2 - \langle u_A^2 \rangle) \frac{\partial^2}{\partial \tau_B^2} (u_B^2 - \langle u_B^2 \rangle) >. \quad (4.3)$$

and u_A and u_B are the components of the velocity at A and B respectively in the direction of the far-field observer at \mathbf{x} . In the case of decaying isotropic turbulence in near incompressible flow at high Reynolds numbers, we may assume that, at any time in the decay, the turbulence is *pseudo-stationary*. Noting also that the operations of averaging and differentiating permute with quantities at B being treated as constants when differentiating with respect to \mathbf{x}_A , and τ_A , and similarly with respect to quantities at A ,

$$U = \frac{\partial^4}{\partial \tau^4} < (u_A^2 u_B^2 - \langle u^2 \rangle^2) >, \quad (4.4)$$

where we define the effective retarded time, $t - x/c_\infty = (\tau_A + \tau_B)/2$, the retarded time separation, $\tau = (\tau_B - \tau_A)$, and $\langle u_A^2 \rangle = \langle u_B^2 \rangle = \langle u^2 \rangle$ is a function of t only. Also $\langle u_A^2 u_B^2 \rangle$ is a

¹The changes in the analysis to include turbulent gases of different density and temperature from that in the ambient medium can be introduced, but then the complete form of T_{ij} must be used, and not the approximation made in deriving Equation(4.1).

function of \mathbf{r} , τ and t . The retarded time separation at the source points can be chosen to find the autocorrelation of the far-field sound intensity, and similarly for the acoustic power.

If $(u_i)_A$ and $(u_j)_B$ are the general components of the velocity \mathbf{u}_A and \mathbf{u}_B respectively, then writing $i = j = 1 \equiv x$ we find $\langle ((u_x)_A^2 (u_x)_B^2) \rangle - \langle (u_x)_A^2 \rangle \langle (u_x)_B^2 \rangle$ can be derived from the general form of the fourth-order isotropic tensor as given by Batchelor(1953). Thus, omitting the dependences on time for convenience only, and writing r_1 for the resolved part of \mathbf{r} in the direction of \mathbf{x} ,

$$P_{xx,xx}(\mathbf{r}) = \langle (u_A^2 u_B^2 - \langle u^2 \rangle^2) \rangle = A(r)r_1^4 + B(r)r_1^2 + C(r) \quad (4.5)$$

where the longitudinal velocity squared covariance

$$\overline{(u_p(\mathbf{x})^2 u_p(\mathbf{x} + \mathbf{r})^2)} - \langle u_p^2 \rangle^2 = r^4 A(r) + r^2 B(r) + C(r), \quad (4.6)$$

and the lateral velocity squared covariance

$$\overline{(u_n(\mathbf{x})^2 u_n(\mathbf{x} + \mathbf{r})^2)} - \langle u_n^2 \rangle^2 = C(r). \quad (4.7)$$

When the turbulence follows Gaussian statistics, as assumed by Proudman(1952), the universal functions $A(r)$, $B(r)$ and $C(r)$ for the fourth-order velocity squared covariances are related to the corresponding functions for the second order velocity covariances, $f(r)$ and $g(r)$, where

$$\overline{u_p(\mathbf{x}) u_p(\mathbf{x} + \mathbf{r})} = u^2 f(r) \quad (4.8)$$

and

$$\overline{u_n(\mathbf{x}) u_n(\mathbf{x} + \mathbf{r})} = u^2 g(r). \quad (4.9)$$

Lighthill(1992) has shown more generally that the fourth-order longitudinal velocity covariance can be replaced by the square of the corresponding second order covariance giving

$$\overline{(u_p(\mathbf{x})^2 u_p(\mathbf{x} + \mathbf{r})^2)} - \langle u^2 \rangle^2 = \left(\overline{u_p(\mathbf{x}) u_p(\mathbf{x} + \mathbf{r})} \right)^2 \left(\frac{\overline{u^4}}{\overline{u^2}^2} - 1 \right), \quad (4.10)$$

and a similar relation holds for the fourth-order lateral covariance by replacing the suffix, p , by the suffix, n . The relationship between the respective fourth and second-order covariances holds for the given time t and the difference time τ . The velocity flatness factor, $T_1 = \overline{u^4}/\overline{u^2}^2$ has the value 3 in Gaussian statistics, and is found by Townsend(1956) to be nearly 3 in decaying isotropic turbulence. A similar result was obtained in the (DNS) results of Sarkar and Hussaini(1993) and Dubois(1993) as presented below. However the joint probability distribution function for the velocity squared at two separated points and for its second time derivative might be expected to

be non-Gaussian and the preliminary results from the above (DNS) results indicate that T_1 in the above formulation should have a value slightly less than 3. However for the purpose of this paper we will use the value T_1 equal to 3 in deriving values of the Proudman constant given below. When the joint probability function is Gaussian, Lighthill's relation reduces to Millionshtchikov's hypothesis as given by Batchelor(1953).

From these results obtained from the Lighthill relationship we find

$$r^4 A(r) + r^2 B(r) = (T_1 - 1) \langle u^2 \rangle^2 (f(r)^2 - g(r)^2), \quad (4.11)$$

and

$$C(r) = (T_1 - 1) \langle u^2 \rangle g(r)^2. \quad (4.12)$$

Noting the points A and B are separated by the vector distance \mathbf{r} , which is in a direction at angle θ to the propagation direction \mathbf{x} , we find from Equation(8), together with Equations(4.10),(4.11) and (4.12),

$$P_{xx,xx}(\mathbf{r}, \tau, t) = (T_1 - 1) \langle u^2 \rangle^2 \left(f(r, \tau) \cos^2 \theta + g(r, \tau) \sin^2 \theta \right)^2, \quad (4.13)$$

with the effective acoustic source function

$$U = \frac{\partial^4}{\partial \tau^4} P_{xx,xx}(r, \tau, \theta). \quad (4.14)$$

In nonstationary turbulence u^2 , T_1 , f and g are also functions of the time t .

If the autocorrelation time difference in the far-field at \mathbf{x} is t^* , then its relation to the retarded time difference in the source region, τ , is

$$\omega t^* = \omega \tau + \mathbf{k} \cdot \mathbf{r}, \quad (4.15)$$

where the wave-number vector in the turbulence is $\mathbf{k} = -\omega \mathbf{x} / (x c_\infty)$. Hence the power spectral density is

$$p_s(\omega) = \frac{\rho_\infty}{8\pi^2 c_\infty^5} \int \int \int \exp(-i\mathbf{k} \cdot \mathbf{r}) d\mathbf{r} \int_{-\infty}^{\infty} \exp(-i\omega \tau) U(r, \theta : \tau, t) d\tau \quad (4.16)$$

and with Equation(17) for U we find, with $k = |\mathbf{k}|$,

$$p_s(\omega) = \frac{\rho_\infty \omega^4}{2\pi c_\infty^5} \int_0^\infty r^2 dr \int_0^\infty \cos \omega \tau d\tau \int_0^\pi \sin \theta \cos(kr \cos \theta) P_{xx,xx}(r, \theta : \tau, t) d\theta. \quad (4.17)$$

If

$$I_1(kr) = \int_0^\pi \sin \theta \cos(kr \cos \theta) \cos^4 \theta d\theta,$$

$$I_2(kr) = \int_0^\pi \sin \theta \cos(kr \cos \theta) \cos^2 \theta \sin^2 \theta d\theta,$$

and

$$I_3(kr) = \int_0^\pi \sin \theta \cos(kr \cos \theta) \sin^4 \theta d\theta,$$

then with Equation(4.13) for $P_{xx,xx}$, the power spectral density becomes

$$p_s(\omega) = \frac{\rho_\infty \omega^4 \langle u^2 \rangle^2 (T_1 - 1)}{2\pi c_\infty^5} \int_0^\infty r^2 dr \int_0^\infty \cos \omega \tau (I_1 f^2 + 2I_2 fg + I_3 g^2) d\tau, \quad (18)$$

noting f and g are functions of r , τ and t only.

In our problem of near incompressible flow, the turbulent Mach number is very small, and in this case we may assume that the modulus of the wave-number k in the turbulence is small and the dependence of I_1 , I_2 , I_3 and p_s on k can then be neglected. We then find the integrals for I_1 , I_2 and I_3 become respectively $2/5$, $4/15$, and $16/15$. Equation(4.18) now takes the simpler form

$$p_s(\omega) = \frac{\rho_\infty \omega^4 \langle u^2 \rangle^2 (T_1 - 1)}{15\pi c_\infty^5} \int_0^\infty r^2 dr \int_0^\infty \cos \omega \tau (3f^2 + 4fg + 8g^2) d\tau. \quad (4.19)$$

The more general case when k is not small requires the values of I_1 , I_2 and I_3 given by

$$I_1(kr) = 2 \left(\frac{\sin kr}{kr} + 4 \frac{\cos kr}{(kr)^2} - 12 \frac{\sin kr}{(kr)^3} - 24 \frac{\cos kr}{(kr)^4} + 24 \frac{\sin kr}{(kr)^5} \right), \quad (4.20)$$

$$I_2(kr) = 2 \left(-2 \frac{\cos kr}{(kr)^2} + 10 \frac{\sin kr}{(kr)^3} + 24 \frac{\cos kr}{(kr)^4} - 24 \frac{\sin kr}{(kr)^5} \right), \quad (4.21)$$

$$I_3(kr) = 2 \left(-8 \frac{\sin kr}{(kr)^3} - 24 \frac{\cos kr}{(kr)^4} + 24 \frac{\sin kr}{(kr)^5} \right). \quad (4.22)$$

Now the relation between $f(r, \tau, t)$ and $g(r, \tau, t)$ in isotropic turbulence must satisfy the equation of continuity, and as shown by Batchelor(1953),

$$g(r, \tau, t) = f(r, \tau, t) + \frac{r}{2} \frac{\partial f(r, \tau, t)}{\partial r}. \quad (4.23)$$

It follows that since $\int_0^\infty (3r^2 f^2 + 2r^3 f \partial f / \partial r) dr = \int_0^\infty \partial(r^3 f^2) / \partial r dr = 0$,

$$\int_0^\infty r^2(3f^2 + 4fg + 8g^2)dr = 2 \int_0^\infty r^4 \left(\frac{\partial f}{\partial r} \right)^2 dr,$$

and then Equation(4.19) becomes

$$p_s(\omega) = \frac{\rho_\infty \omega^4 \langle u^2 \rangle^2 (T_1 - 1)}{c_\infty^5} \frac{2}{15\pi} \int_0^\infty \cos \omega \tau d\tau \int_0^\infty r^4 \left(\frac{\partial f}{\partial r} \right)^2 dr. \quad (4.24)$$

The fact that a significant part of the equivalent acoustic source function, $r^2(3f^2 + 4fg + 8g^2)$, integrates to zero for all values of f has important consequences for the generation of noise from turbulent flows.

In many cases we require the complete acoustic source distribution function, $r^2(3f^2 + 4fg + 8g^2)$, which includes that portion which, on integration over all values of r , makes zero contribution to the acoustic power. The complete acoustic source function as well as its positive only contribution to the acoustic power are given in the examples below. We see that the power spectral density, $p_s(\omega)$, as given by Equation(4.24), has its dominant contribution far removed from the origins of r and τ , where the longitudinal velocity correlation function has its maximum value. This reflects on the poor efficiency of the conversion of the flow kinetic energy into acoustic energy, since away from the origins of r and τ , the magnitude of the function $\partial f / \partial r$ will be extremely small. We are reminded that our result is based on the assumption of *pseudo-stationary* turbulent flow. In decaying isotropic turbulence the local characteristic velocity, $u = \sqrt{\langle u^2 \rangle}$, the length scale, L , and the time scale, $1/\Omega$, are all functions of the decay time.

We cannot proceed without introducing a distribution for $f(r, \tau, t)$. We noted that the integral in Equation(4.24) is dominated by the values of the integrand at r and τ away from the origin, and where $f(r, \tau, t)$ is a very small quantity. Thus we may assume, to a good approximation as discussed in Section(3) above, the distributions of r and τ are independent, so that

$$f^2(r, \tau, t) = \psi(\Omega \tau) \exp\left(-\frac{\pi}{2} \frac{r^2}{L^2}\right), \quad (4.25)$$

where $L = \int_0^\infty f(r, 0, t)dr$ is the local integral scale and Ω is the local reference frequency, proportional to the peak frequency in the turbulence. Both L and Ω are functions of time in the case of turbulent decay. In the stationary case they are constants. The distribution assumed for $f(r, \tau, t)$ in Equation(4.25) is its self-preserving form, which is independent of time during the decay. The change in the longitudinal velocity correlation function during the decay is dependent on the variations of L and Ω with time. We find it convenient to define, as above, the characteristic velocity in the turbulence as $u = \sqrt{\langle u^2 \rangle}$, and the reference Strouhal number as $S_T = \Omega L / u$, which we assume is constant throughout the turbulence and is independent of time throughout the decay. The time separation dependence in the two-point velocity space-time scalar function, $f(r, \tau, t)$ has been chosen to establish a far-field noise spectrum proportional to $\omega^4 / (1 + (\omega/\Omega)^2/4)^3$. Such a spectrum function, already discussed in Section(3) above and shown in Figure(2), is found to be similar to the acoustic spectrum as found in the (DNS) results. The frequency at the peak in the noise spectrum, ω_m , is $\sqrt{8}\Omega$. The (DNS) results are also plotted in Figure(1), where it is shown

the spectrum changes from nearly ω^2 at low frequencies to ω^{-2} at high frequencies. However since the total acoustic power is proportional to the fourth time derivative of T_{xx} we have chosen the low frequency dependence proportional to ω^4 rather than ω^2 . The corresponding temporal covariance is shown in Figure(3) with the (DNS) results of Dubois(1993). The frequency at the peak in the acoustic spectrum is slightly greater than that corresponding to the turbulent energy spectrum. Thus the eddies responsible for the dominant contribution of the acoustic spectrum are slightly smaller in scale than the energy containing eddies.

Hence the total acoustic power is found by integrating Equation(4.24) over all values of the frequency, ω . If we put $f(r, 0, t) = f(\chi) = \exp(-\pi\chi^2/4)$, where $\chi = r/L$, then the result is

$$p_s(t) = \frac{32}{15}(T_1 - 1)\frac{\rho_\infty u^8 S_T^4}{c_\infty^5 L} \int_0^\infty \chi^4 \left(\frac{df}{d\chi}\right)^2 d\chi. \quad (4.26)$$

Thus the value of the Proudman constant, α , in

$$p_s(t) = \alpha \frac{\rho_\infty u^8}{L c_\infty^5}, \quad (4.27)$$

is

$$\alpha = \frac{32}{15}(T_1 - 1)S_T^4 \int_0^\infty \chi^4 \left(\frac{df}{d\chi}\right)^2 d\chi. \quad (4.28)$$

We find

$$\int_0^\infty \chi^4 \left(\frac{df}{d\chi}\right)^2 d\chi = \frac{15}{4\sqrt{2}\pi} = 0.8440, \quad (4.29)$$

and finally

$$\alpha = 1.80(T_1 - 1)S_T^4, \quad (4.30)$$

which is the important result obtained from this section.

Thus the Proudman Constant, α , depends on the flatness factor, T_1 and the fourth power of the turbulent Strouhal number, S_T .

It also confirms that the source of the acoustic power, which is proportional to the fourth time derivative of the retarded time covariance of T_{xx} , is positive for all values of r and τ . However as noted above this is mainly due to a large part of the volume integral of the T_{xx} covariance being exactly zero. The spatial correlation volume of the equivalent acoustic source depends on $(f')^2$, and is equal to $0.8440L^3$ as shown in Equation(4.29). As expected the equivalent correlation length, $0.945L$, is slightly smaller than the scale of the energy containing eddies. The peak in the acoustic source distribution function occurs at $\chi = 1.3820$.

When the Strouhal number of the turbulence, $S_T = 1.25$ we find that $\alpha = 4.4(T_1 - 1)$ and when the flatness factor, $T_1 = 3$ as found in the (DNS) results discussed below, then $\alpha = 8.8$. Clearly the value of α depends on S_T , and although we know S_T is of order unity, its value cannot be determined from our analysis. When $S_T = 1$ and $T_1 = 3$ we find $\alpha = 3.6$. If $f(r/L) = \exp(-r/L)$ in place of $f(r/L) = \exp(-\pi r^2/4L^2)$, covering possibly the range of likely distributions between low and high Reynolds numbers, then with these same values of S_T and T_1 the value of $\alpha = 3.2$. Thus all we can say here is that, covering the range of low to high Reynolds numbers, α is likely to be in the range 3 to 9, provided S_T is in the range 1 to 1.25. These values of α are in close agreement with those given by Proudman(1952) if S_T has a value of around 1.25. This applies also to our re-calculation of those results and in a revised analysis, in which the retarded-time is not neglected until the conclusion of the analysis, as shown in Section(2). The lower value of α also equals the same order of magnitude as that obtained from the (DNS) simulations, as shown below, provided S_T has the value unity. When this investigation was started it was assumed that one of the outcomes would have been that the (DNS) results would provide a calibration for the turbulent Strouhal number, S_T . This remains a possibility although first it is necessary to establish that the (DNS) results discussed below are an accurate guide to the evaluation of α at high Reynolds numbers and that these simulations do not show any contamination resulting from any inadequate resolution in both space and time of both large and small scale motions. So far it has been possible to establish that, as expected, S_T has a value of order unity, and appears to have values in the range 1.0 to 1.25.

Now during the decay

$$\frac{dK}{dt} = -\epsilon, \quad (4.31)$$

where the kinetic energy, $K = 3 \langle u^2 \rangle / 2$, and the rate of dissipation, $\epsilon \propto \langle u^2 \rangle^{3/2} / L$. If we assume $L(t) \propto t^n$ and $\langle u^2 \rangle \propto t^{-s}$, then we find from the Eddy Damped Quasi-normal Markovian(EDQNM) results of Lesieur(1990), that $n = 0.31$ and $s = 1.38$. If we use these results, then the acoustic power, p_s , falls as $t^{-5.83}$, and is in fair agreement with the results of the (DNS) simulations. Additionally we find that $L/u \propto t^{(2n+s)/2} \propto t$ for all values of s and n , and hence Ω decreases with time according to t^{-1} . Thus the turbulent Strouhal number, S_T , is independent of time in the decay, consistent with the assumption made previously. In full self-preserving flow with $s = 1.0$, and $n = 0.5$, we find p_s falls as $t^{-4.5}$. All these results apply when the velocity and the velocity derivative flatness factors remain constant during the decay.

Before we leave this section we might reflect on the result had we completely ignored retarded times in the evaluation of Equation(2.2). Then the sound power per unit volume would be given by the simultaneous fourth time derivative of the fourth order velocity covariance, all evaluated at the same time, t . However we define U as in Equation(2.3), but with τ replaced by t since τ has been put equal to zero. In self-preserving flow we then find the time differentiation operates only on the product of u^4 and L^3 , with the result

$$p_s(t) = (T_1 - 1) \frac{\rho_\infty}{6c_\infty^5} \frac{d^4}{dt^4} (u^4 L^3) \int_0^\infty \chi^4 \left(\frac{df}{d\chi} \right)^2 d\chi. \quad (4.32)$$

From Equation(4.32) we find that the acoustic power output depends critically on the decay laws for u and L , especially in the initial stages of the decay. But the result, as might have been expected

since the random temporal characteristics of the turbulence are now ignored, gives a much lower sound power than that given by Equation(4.30).

5. Comparison with the Direct Numerical Simulations(DNS) of Isotropic Turbulence by Sarkar and Hussaini(1993), and Dubois(1993).

The (DNS) results are presented here in some detail, with the permission of the authors, in order to make a detailed comparison between the results and assumptions made in the simulations and in the analysis presented in Section(2) above.

(i) The computational range.

These (DNS) results from the modelling of isotropic turbulence were performed for an initial Taylor microscale Reynolds number, R_λ , of 65 and a Mach number, based on the root mean square of the turbulent velocity, equal to 0.05. (The value of R_λ quoted by Sarkar and Hussaini was 50, but this was based on the turbulent velocity, $q = 3\sqrt{\langle u^2 \rangle}$, and $\lambda = q/\sqrt{\langle \omega^2 \rangle}$ whereas we define R_λ based on $\lambda^2 = 15\nu \langle u^2 \rangle / \epsilon$.) A 64^3 spatial grid was used with a time step Δt equal to $0.00275(K/\epsilon)_0$. Twenty such simulations were performed and each simulation was conducted up to $t = (K/\epsilon)_0$, where $(K/\epsilon)_0$ is the initial eddy turnover time. During these simulations the turbulence decayed and the Taylor microscale Reynolds number fell to values approaching 20 over one initial eddy turnover time. The simulations were then stopped for with such low values of the Taylor microscale Reynolds number the energy containing scales of the turbulence approach the Taylor microscale, and the dynamics of the turbulence change markedly from its characteristics associated with higher Reynolds numbers. At less than $R_\lambda = 48$ approximately, the peak frequency in the acoustic spectrum exceeds the frequency associated with the Taylor microscale eddies. Thus for these simulations with the initial value of $R_\lambda = 65$, we might expect the results to display some characteristics for the acoustic power output different from the analytic results of Proudman and the results given in this paper, which are based on the assumption of a high Reynolds number, where the results are independent of Reynolds number. The explicit dependence on Reynolds number of the acoustic power output from isotropic turbulence is a subject that so far has not been investigated, although it has frequently been assumed that for values of about $R_L > 1000$, where $R_L = uL/\nu$, the variations with Reynolds number are likely to be small.

(ii) The variation of K , ϵ and $f(r/L)$ during the decay.

The results of Sarkar and Hussaini(1993) are plotted and compared with the theoretical results. Figure(8) shows the decay of turbulent kinetic energy as a function of non-dimensional time, $t(\epsilon/K)_0$ and Figure(9) shows similar results for the dissipation function. It is found that the decay of turbulent kinetic energy, in these simulations, follows $t^{-1.38}$ except near the initial decay period. It is also found that the dissipation function falls as $t^{-2.38}$ except in the initial period of decay, where it first increases rapidly to a maximum value and then falls. These results for non-dimensional times greater than 0.4 are in agreement with (EDQNM) theory as presented by Lesieur(1990). The

present results of Sarkar and Hussaini(1993) for the decay of K/K_0 and ϵ/ϵ_0 are similar to the previous results of Herring et al(1973), for the same initial energy spectrum, but display different values for the peak in the dissipation function. It is possible that the earlier results were much less well resolved than the data obtained by Sarkar and Hussaini(1993). The present (DNS) results also differ from the experiments of Comte-Bellot and Corrsin(1966) who found $K \propto t^{-1.26}$ and Warhaft and Lumley(1978) who obtained $K \propto t^{-1.34}$. In fully self-preserving turbulence $K \propto t^{-1}$ and $\epsilon \propto t^{-2}$, with both λ and L being proportional to $t^{1/2}$. Figure(10) shows the fall in R_λ with time and again the agreement with the results from (EDQNM) theory is fair for times greater than 0.4. Figure(11) shows the comparison between the (DNS) results and the experimental results of Stewart and Townsend(1951) in grid turbulence, for the longitudinal velocity correlation function, $f(r/L)$. The latter results have been corrected to provide the expected distribution appropriate to very high Reynolds numbers. No attempt has been made to make a similar correction to the (DNS) data to allow for the effects of the low Reynolds number. Clearly the comparison is sensitive to the value chosen for the integral length scale L . The (DNS) results provide values of $L = (3\pi/4) \int_0^\infty (E(k)/k)dk / \int_0^\infty E(k)dk$ as well as the component values L_{uu} , L_{vv} and L_{ww} . Since the (DNS) results for $f(r)$ at small values of r approximate to a Gaussian distribution, we find it more convenient to select a value for L such that $f(1) = 0.4559$, since $f(r/L) = \exp(-\pi/4(r/L)^2)$ is a fair fit with the data in the region $0 < r/L < 1$. This is the longitudinal velocity correlation function for an unbounded flow in the initial stage of decay, when the initial energy spectrum function, $E(k) = k^4 \exp(-2k^2/k_m^2)$. In most of the (DNS) results described here $k_m = 6$. In the high Reynolds number experimental results of Stewart and Townsend $f(r/L) \simeq \exp(-r/L)$ in $0 < r/L < 1$. The low Reynolds number (DNS) results are at variance with these experimental results at separations $r/L \leq 1$, and are notably smaller at larger separations. If the comparison between the (DNS) results and experiment had been made at the same Reynolds number the agreement between them would have been shown to be much closer. A feature of the (DNS) longitudinal velocity correlation curve is the 'shallow bump' in the region of $3 < r/L < 4.5$. At such large spatial separations, the magnitude of the correlation function, $f(r/L)$, is very small but not negligible. The corresponding transverse correlation function, $g(r/L)$, is negative in this region. As first noted by Townsend(1956) this feature of a 'shallow bump' at large spatial separations can, in certain cases, be interpreted as the existence of a large scale structure in the turbulence having a non-negligible fraction of the turbulent kinetic energy. Such structures, generally referred to as regular or coherent structures, are a feature of turbulent shear flows, and are a direct result of the flow boundary conditions. Experiments on grid turbulence do not show such features.

(iii) The variation of λ and L during the decay.

Figure(12) shows for the 128³ simulation the variation of λ^2 with $t\epsilon_0/K_0$. The expected linear variation is found when $0.4 \leq (t\epsilon_0/K_0) \leq 0.8$. The variation of L_{uu} with time is shown in Figure(13). The same figure shows the comparison of L_{vv} with L_{ww} . The expected variation with time for L_{uu} in isotropic turbulence is found between non-dimensional times of 0.4 to 0.8, and in this same window, $L_{vv} = L_{ww}$. Here suffix uu denotes the longitudinal scale and vv and ww denote the transverse scales. But in unbounded turbulence we expect $L_{uu} = 2L_{vv} = 2L_{ww}$ and this relationship is not found at any time in the decay. Thus in these simulations the negative values of the transverse correlation function, $g(r)$, appear to be inadequately resolved. Other (DNS) simulations performed by Sarkar and Hussaini(1993) for smaller values of L_{uu}/D show better resolution for $g(r)$ at large values of r/L in the range of negative values of $g(r)$. In these latter results $g(r)$ develops a periodic pattern becoming successively negative and positive with a very small amplitude of about 0.01.

The first negative loop, on the other hand, has an amplitude of nearer 0.1.

(iv) The variations of skewness and flatness during the decay.

Figure(14) shows the variation of the velocity derivative flatness and skewness factors with time during the decay. In the region from non-dimensional times of 0.4 to 0.8 the skewness factor, S_2 , is -0.53 and the flatness factor, T_2 , is 4.0 , but the velocity flatness factor takes on the value $T_1 = 3$ as found in experiments.

(v) The changes in $f(r/L)$ resulting from periodic boundary conditions in the (DNS) results.

In the 128^3 simulations the Kolmogoroff length scales are not resolved and the Taylor microscale is approximately twice the grid dimensions. Initially the energy containing scales were 1.25 times the Taylor microscale. In the simulation the energy containing scales grow by a factor of about 1.5 times their initial value, and the Taylor microscale eddies first decrease in size and then increase back towards their initial value. The initial energy wave-number spectrum is defined as $E(k) = k^4 \exp(-2(k/k_m)^2)$ and the velocity has a Gaussian joint probability density function. With a low wave-number spectrum proportional to k^4 we might expect, as a result of the near permanence of the big eddies, that this spectrum would be retained throughout the decay. However with the use of homogeneous boundary conditions and noting that $D/2L$ is of order 5 for the 64^3 and 7 for the 128^3 simulations, where D is the size of the computational domain, the large eddies responsible for the low frequency part of the spectrum will be strictly limited to eddies of scale equal to half the width of the computational domain and the number of such eddies will be strictly limited. Thus in comparison with unbounded turbulence, at higher Reynolds numbers, (DNS) can only partly resolve the large eddies responsible for the low frequency part of the spectrum. An important feature of the (DNS) results is that at low to moderate Reynolds numbers the use of periodic boundary conditions imposes restrictions on the asymptotic form of the longitudinal velocity correlation function, $f(r)$, since it is a periodic function and is symmetric with respect to the centre of the computational domain. It is therefore a function unlike that used in the theoretical analysis which satisfies the asymptotic conditions of approaching zero at large values of r . Some recent (DNS) calculations of Dubois(1993) in the same Reynolds number range as in the results of Sarkar and Hussaini(1993), but where the turbulence is forced to prevent the rapid fall in kinetic energy with time as found in unforced isotropic turbulence, show that although the characteristics of the longitudinal velocity correlation function, $f(r)$, at small separation distances, r , are similar to those found by Sarkar and Hussaini(1993), at larger separations the function deviates greatly, being highly dependent on the forcing frequency, the value of which dominates the low frequency part of the spectrum at all times in the decay. The magnitude of the forcing energy $f \cdot u$ also has a strong influence on the characteristics of the longitudinal velocity correlation function at large separation distances. With strong forcing the longitudinal velocity correlation function does not tend to zero when $r \rightarrow D/2$, a distance equal to the half-width of the computational domain. Its value is a function of the forcing amplitude. The (DNS) 96^3 computations of Dubois(1993) show that changing the wave-number of the forcing, from an even to an odd wave number changes the sign of the longitudinal velocity correlation function at large separations. An immediate conclusion is the apparent sensitivity of $f(r)$ to changes in the boundary conditions and consequent changes to the large

eddy structure within the computational domain. The results of Sarkar and Hussaini(1993) show little change between their 64^3 simulations compared with their 128^3 simulations, but the Reynolds numbers are similar and changes in the grid size appear to be insufficient to effect changes in the behaviour of $f(r)$ at large separations in r . The results of Dubois(1993) in which the forcing is made very weak generates values of $f(r/L)$, as shown in Figure(11), in good agreement with the results of Sarkar and Hussaini(1993) at small spatial separations but show marked differences at large separations. The results of Dubois for the longitudinal velocity correlation function, at large separations, follow more closely a Gaussian distribution as expected at very low Reynolds numbers. (These differences between forced and unforced turbulence simulations are not surprising although it cannot be explained why the forced results follow more closely the Gaussian distribution at large separations than the unforced results.) When the forcing is increased, marked changes occur to the function $f(r/L)$. However when the effect of the forcing is removed the function reduces to approximately that of the Gaussian distribution as found for weaker forcing. However a positive conclusion from this work is that both the forced and unforced (DNS) at similar Reynolds numbers have similar longitudinal velocity correlation functions at small separation distances and around the distance $r = L$, where the energy containing scales are likely to make a dominant contribution. The shape of this correlation curve in this region $r/L < 1$ is typical of the results for low to moderate Reynolds number but differs markedly from the the higher Reynolds numbers of Stewart and Townsend(1951), as shown in Figure(11). Since a conclusion of this work is that the noise generated is dominated by the contribution made by the energy containing scales, there appears some justification in choosing the distribution $\exp(-\pi/4(r/L)^2)$, as used in the calculations for the acoustic power made above. This has the merit of representing the (DNS) results near $r = L$, and satisfies the necessary conditions at $r = 0$ and $r = \infty$. As shown in Figure(11). such a distribution function is a poor representation, of the results at high Reynolds numbers, at both small and large separation distances, but we note these results only apply when the time separation effects are equal to zero. When the full space-time separation effects are considered, however, then we find from the (DNS) results of Dubois(1993) that the approximate spatio-temporal independence and self-preserving form of the fourth order covariance used in Equation(3.5), gives a reasonable fit to the computed longitudinal velocity correlation function at moderate to large values of the space separation, r , and the time separation, τ , and especially around those values equal to the scales of the energy containing eddies. Such a result is likely to apply over a wide range of Reynolds numbers, and well outside the limits of the (DNS) range of Reynolds numbers.

So far we have discussed the features of the low wave-number spectrum and its influence on the longitudinal velocity correlation function. Its high wave-number spectrum rapidly changes, from its imposed spectrum at time $t(\epsilon/K)_0 = 0$, since as time advances the nonlinear interactions result in populating the higher frequencies, and the production of small scales of turbulence down to the Kolmogoroff dissipating scale, k_s . At the low to moderate Reynolds numbers in these (DNS) results an inertial subrange, with $k_L \ll k \ll k_s$, cannot exist with a near $k^{-5/3}$ spectrum. The $k^{-5/3}$ spectrum in the inertial sub-range would only exist at much higher Reynolds numbers where the ratio between L and λ was at least greater than 10. In the 64^3 simulations the dissipating range of eddies is not fully resolved. Sarkar and Hussaini(1993) do include a 128^3 simulation and although this simulation resolves the Kolmogoroff scales it cannot resolve all the eddies in the dissipation range. However it appears to improve the resolution of the larger scales. But a comparison between the results from both simulations shows that the differences between them are small, at least for the calculated acoustic power output.

(vi) The acoustic power distribution.

Fig(15) shows the acoustic power distribution as predicted according to the method described in Section(4) and in particular to the contribution to the Proudman constant, α , as a function of the nondimensional spatial separation distance, r/L . The acoustic power distribution is comprised of three functions two of which are positive quantities, whereas the third is negative. When integrated with respect to r/L the first function, which peaks at $r/L = 0.56$, when combined with the negative function, which peaks at $r/L = 1.38$, is exactly zero. The remaining function, which also peaks at $r/L = 1.38$, is positive and is the only contribution to the acoustic power. The value of the Proudman constant, corresponding to the results given in Figure(15) is $\alpha = 3.6$. The values for the Proudman constant, using Proudman's equation was $\alpha = 12.5$ (Proudman gives the value 13.5) and from our revised equation $\alpha = 11.0$. The peak values in both estimations occur at $r/L = 0.8$ approximately. Proudman's results, which make no assumptions as to the value of the turbulent Strouhal number, as shown in Figure(16), give an acoustic power distribution which is similar to that found by us in Section(2), although the peak values differ by a factor of about 3, if we assume a flatness factor of 3, and a turbulent Strouhal number of unity. The differences in these values of the Proudman constant can be explained in terms of changing the values of the turbulent Strouhal number from 1 to 1.25. However we cannot overlook the fact that the (DNS) results have shown that, to a good approximation, the turbulent Strouhal number is approximately unity throughout the decay. A value of α between 3 and 4.5 is in fair agreement with the results obtained from the first (DNS) method used by Sarkar and Hussaini(1993). They obtained an average value of $\alpha = 2.6$, with a value of $\alpha = 3.5$ near the commencement of the true decay, when the Reynolds number was highest, falling to $\alpha = 1.6$ near the end of the simulation when the Reynolds number was very small. At these low Reynolds numbers the energy containing scales and the Taylor microscales overlapped. In the second (DNS) method used by Sarkar and Hussaini(1993), they evaluated the two-point longitudinal velocity correlation function, $f(r, t)$, and the second time derivative covariance of the Lighthill function T_{ij} as a function of spatial separation and the corresponding contribution to the acoustic power distribution. *This calculation represents the first occasion that a direct calculation of the second time derivative covariance of T_{ij} has been attempted.* The results are compared with those obtained from our model in Figure(17). We see the large peak values obtained in the (DNS) simulations where the values peak near the origin. However the value of the Proudman constant obtained from this result is $\alpha = 2.8$, which is close to that found in our model. This result, which was obtained at a nondimensional time of $T = 0.55$, where $T = t\epsilon_0/K_0$, was quoted by Sarkar and Hussaini(1993) as giving a value equal to that obtained by their first method, which as stated above has the average value $\alpha = 2.6$. The overall accuracy of the (DNS) results in calculating the acoustic power distribution has not been determined, but our results from Section(2) show the extreme difficulty to be expected in obtaining an accurate answer to the acoustic power distribution when, as we have shown in Section(2), the dominant part of the distribution near the origin integrates to zero as shown in Figure(15).

(vii) The comparison between the second and fourth-order covariances.

Independently Sarkar and Hussaini(1993) and Dubois(1993) have established the correctness of the Lighthill relationship given in Equation(4.10) above, although the numerical results infer a slightly lower value for the multiplying factor (flatness factor minus unity) than the measured values of flatness factor as found by Townsend(1956) for the velocity, and as found in the present (DNS)

results, both of which gave values near 3. It might have been expected that the flatness and skewness factors for the velocity squared would differ from those of the velocity alone, but the (DNS) results clearly show a value for T_1 just below 3 over the complete time of the simulation. The results of Dubois(1993) are plotted in Figures(18) and (19), respectively, for various temporal and spatial separations and convincingly show that with $T_1 = 3$ the measured and predicted values of the fourth order velocity covariance are in close accord. Similar results were obtained for the transverse covariance. In all the results quoted above for the Proudman constant we have used a value of 3 for the flatness factor, T_1 .

(viii) The turbulent Strouhal number.

We have shown above the importance of the turbulent Strouhal number, $S_T = L\Omega/u$, in the determination of the characteristics of the noise generated from turbulence. The results of both Sarkar and Hussaini(1993) and Dubois(1993) show S_T has a value of order unity. However in both works Ω has not been measured directly as, say, the inverse integral time scale of the turbulence in the decay. A difficulty is that Ω is directly related to the ratio, u/L , which is the inverse of the local eddy turnover time. This is similar in magnitude, at low Reynolds numbers, to the total time of the simulation before the turbulent Reynolds number drops to unacceptably low values. In the present simulations the total computation time is of order 3 to 5 times the local eddy turnover time. Thus we cannot find reliable values for Ω from the present (DNS) simulations of Sarkar and Hussaini(1993) for unforced turbulence, due to the difficulty in extracting the effects of the time decay from the time separation effects. An approximate analysis of the data shows that $\Omega \approx u/L$, corresponding to a value of $S_T = O(1)$. If we turn to the (DNS) results of Dubois(1993) for the case of forced turbulence during the decay, where the kinetic energy remains almost constant we find an excellent fit with the acoustic power time covariance derived from the measured acoustic spectrum of Sarkar and Hussaini(1993) shown in Figure(2). The comparison is given in Figure(3) where the time covariance data from the results of Dubois only show some deviation at large values of the separation time, τ . However the data, as obtained in the simulations, is adversely affected, at large time separations, by the degree of forcing and this part of the data has been ignored. (Since the degree of forcing affects the integral length scale, L , we have selected a value which is consistent with our choice of $f(r/L)$, and the position of the minimum in the transverse correlation function, $g(r/L)$.) The result of this comparison is that $\Omega \approx 1$, when $u/L = O(1)$, in confirmation with the result suggested from the Sarkar and Hussaini(1993) data, and in line with the value of $S_T = 1$ as used in the results presented above. However the overall accuracy of our method of deriving a value for the turbulent Strouhal number, S_T , from the (DNS) results can at best be taken as an order of magnitude estimate only, and these values may be shown to be inappropriate for isotropic turbulence at higher Reynolds numbers. It might be noted, that in predictions of noise generated from shear flow turbulence, values of $S_T = 1.25$ to 1.75 have been used to calibrate these with experimental data. If we had used the 'uncorrected' integral length scales from the (DNS) data of Dubois(1993), then we would have obtained values for the turbulent Strouhal number in this same range.

(ix) Summary.

At the Reynolds numbers used in the (DNS) calculations of Sarkar and Hussaini(1993), the ratio of the integral length scale, L , to the half width of the computational domain was initially 0.14 and increased to 0.21 towards the end of the simulation. Thus we might expect to see some interference on the two-point velocity covariance at large spatial separations as a result of the finite size of the computational domain and the use of periodic boundary conditions. Such conditions are unlikely to affect greatly the global characteristics of the turbulence, as confirmed by previous (DNS) simulations. However their effect on $f(r)$ and $g(r)$ is not negligible and will have important repercussions on the characteristics of the noise generated. In Section(2) we showed the noise generated depended on the distribution of $r^2(3f^2 + 4fg + 8g^2)$ and in particular its values at the larger spatial separations. Moreover, due to the dependence of $g(r)$ on $f(r)$, a large portion of this distribution, when integrated to find the total acoustic power, has a value of exactly zero. In fact the total acoustic power is a function of the square of the derivative of the longitudinal velocity correlation function, and small deviations in the shape of the longitudinal velocity correlation function, will change the acoustic source function by a significant amount. Of equal importance is the need to consider the complete space-time properties of the velocity and the velocity squared covariance and not just their distributions with respect to space and time separately. The problem is compounded by the fact that the T_{xx} covariance, involving, in the case of turbulence at low Mach numbers, the velocity squared covariance, is itself of small magnitude in the region of those values of r , and τ , which contribute most to the acoustic power generated per unit volume of the turbulence. Of course the acoustic power output is proportional not to the covariance of T_{xx} but to $\partial^2 T_{xx} / \partial \tau^2$, and this covariance is not negligibly small. One must therefore provide adequate time and space resolution over all space and time separations, and especially at large separations, for the accurate computation of these covariances and their derivatives, and thus of the generated noise. It is this that makes it such a challenging task in all numerical simulations, and equally in any attempted future experiments. Sarkar and Hussaini(1993) have tackled all these problems in their pioneering study with notable success. It is clear however that further work is needed to clarify some of the differences which remain between the numerical and analytic investigations, and their extension to higher Reynolds numbers.

At higher Reynolds numbers, where the size of the computational domain is very large compared with both the energy containing eddies and the dominant larger eddies, of length scale many times L , the effects discussed above are likely to have only a small influence on the characteristics of the turbulence. From the (DNS) computations discussed here, it would appear separation distances of at least 8 to 10 energy containing scales are required to minimise this interference. In the present (DNS) computations such a distance is more than half the size of the computational domain, and it would appear the characteristics of the turbulence, especially in the larger scales will be influenced by their interaction, which is an interaction not present in isotropic turbulence free from periodic boundary conditions. A simple way to describe this influence of the periodic boundary conditions at low Reynolds numbers is to assume, that as a consequence, there exists a class of weak large eddies within the computational domain of size of order half the width of the computational domain. Their effect on the physical characteristics of the turbulence may not be great for large enough values of R_L and R_λ , but their effect on noise generation would appear to be non-negligible owing to two important factors. These are the resulting non-uniformity of $f(r)$ throughout the computational domain, and the fact that the noise generation depends on the derivative squared of $f(r)$, where changes in its distribution are more sensitive than for $f(r)$ itself. At higher Reynolds numbers these problems are likely to largely disappear for then the asymptotic form of $f(r)$ is reached

at distances small compared with the half-width of the computational domain. Thus when the number of energy containing eddies within the computational domain is large enough and averages are obtained in a volume of the computational domain at a sufficient distance from the periodic boundaries, then the influence of the periodic boundary conditions is expected to be negligible. In the present work of Sarkar and Hussaini(1993) the overall interference effects arising from periodic boundary conditions and the relatively low Reynolds number of the simulations, are found to be not negligible and hence we must allow for some, albeit small, low Reynolds number effects in these (DNS) simulations when comparing them with the asymptotically high Reynolds results of Proudman(1952) and the results presented here. In addition the finite intensity of the turbulence at the domain boundaries is a problem that needs further careful consideration in any future work on this same problem. A higher order (DNS) simulation is desirable but is not currently available. The alternative is to use a Large Eddy Simulation(LES) and work on these lines has recently been published by Witkowska et al(1993).

We have discussed above the need for high orders of resolution in both space and time in deriving the fourth time derivative of the Lighthill stress tensor T_{ij} . We have seen we require its value at all values of space and time separation and not only at either small or large values separately. The analysis in Section(2) has shown the extreme sensitivity in this function to small changes in the value of the longitudinal velocity covariance. The analysis, however, cannot predict a value for this function and we are therefore fortunate in having, for the first time, values obtained from the (DNS) calculations of Sarkar and Hussaini(1993). As shown above these latter results even though obtained at low values of the turbulent Reynolds number nevertheless provide important information with respect to the fourth-order covariance of T_{ij} and its fourth time derivative. Using the results of Sarkar and Hussaini(1993) for the two-point velocity covariances we are able to obtain an independent check on the accuracy of the (DNS) simulations. Our fair agreement with the estimates of the total acoustic power as found by Sarkar and Hussaini(1993) may be fortuitous, but the indications are that the effects of Reynolds number may be fairly small, although the changes in the velocity covariance at large spatial separations, resulting from test examples where the integral scales were no longer negligible compared with the size of the computational domain, need further investigation. Of more concern are the differences between the computational and analytic results in the shapes of the acoustic power distribution with spatial separation. Our analytic results based on the (DNS) results for the two-point velocity covariance, give values for the fourth-order covariance and its fourth time derivative that follow the trends of our results obtained in Section(2). These analytic results show clearly the dependence of the square of the derivative of f on the acoustic power distribution, but this result is not obtained from the data obtained by Sarkar and Hussaini(1993) from their evaluations of the second time derivative covariance of T_{ij} . Sarkar and Hussaini(1993) neglect retarded time in their evaluation of this covariance, but in the light of the small difference found between our calculations and those of Proudman(1952), it seems unlikely this would be a major source of error in these low Mach number calculations. However the fourth time derivative of the T_{ij} covariance does require high resolution, as suggested by the results shown in Figures(3) and (7) for the time separation correlation function and its fourth derivative respectively. Sarkar and Hussaini(1993) devoted much attention to achieving that high order of accuracy by the use of a third order Runge-Kutta time integration scheme with an extremely small time step. Further work needs to be done however to establish the accuracy of this scheme. It should be noted that when simultaneous time derivatives, together with ensemble or volume averages, are taken the operations permute and we are left with an expression for the total acoustic power similar to that given in Equation(4.32) when the turbulence is both decaying and self-preserving. This formula gives a reduced value for the total acoustic power, and illustrates the

extreme care needed in evaluating the Lighthill Integral, especially when introducing any form of approximation. There is no evidence this has occurred in the work of Sarkar and Hussaini(1993) but it is a warning to all future investigators.

4. Conclusions

In 1952, Proudman applied Lighthill's theory of Aerodynamic Noise to the case of the radiated noise from isotropic turbulence in near incompressible flow or flow at low Mach numbers. This fundamental example of aerodynamic noise should be regarded as a 'benchmark' against which the results from numerical studies of turbulence can be compared under similar flow conditions, using the methods of Direct Numerical Simulation (DNS) or Large Eddy Simulation (LES).

The results obtained by Proudman for the total acoustic power output per unit volume of turbulence are compared with those obtained by a direct evaluation of the Lighthill T_{ij} covariance. We use the relationship between the resulting fourth-order covariance and the similar second-order covariance as first proposed by Lighthill(1992), and in which no statistical assumptions are made. The relationship is found to be in good agreement with results obtained from (DNS) calculations. The results obtained by this method are in fair agreement with the earlier results of Proudman, and the re-evaluated results presented here. However in our method a free parameter is the turbulent Strouhal number, S_T , and its value can only be obtained, say, by comparison with the (DNS) results. These results suggest its value is of order unity. To obtain agreement between our results and those of Proudman, however, we need a value of S_T of approximately 1.25. The recent results (DNS) results of Sarkar and Hussaini(1993) when compared with the analytic solutions suggest a value for S_T of about unity. The (DNS) results are obtained for an initially moderate, to low, Reynolds number, R_λ , where the difference between the length scales of the energy containing eddies and the Taylor microscale eddies is less than a factor of 10. In spite of this restriction, the results for the far-field acoustic spectrum have the characteristics of noise generated at higher Reynolds numbers, and it is unclear whether or not a significant Reynolds number effect is present when the results for the total acoustic power output are being compared. Some differences exist between our results and those of Proudman, and the (DNS) results of Sarkar and Hussaini(1993), and suggest that in spite of the high resolution in space and time achieved, the demand is for still higher accuracy in calculating numerically the fourth time derivative of the T_{ij} covariance and its space time properties. It is hoped that these results will assist in guiding further research in the field of computational aeroacoustics involving the noise radiated from turbulence, and help to clarify the small differences which remain between these several treatments of the problem of the noise radiated from isotropic turbulence. Overall it is found that the numerical simulations are capable of reproducing to a good approximation the flow physics of aeroacoustics involving turbulent flows.

Acknowledgements

The author wishes to express his thanks to Dr. M.Y. Hussaini for the opportunity to perform this work at ICASE and to Dr. S. Sarkar and Dr. M.Y. Hussaini for making their results on the 64^3 and the 128^3 (DNS) numerical simulations available for comparison with the analytical results presented in this paper. Thanks are also due to Dr. T. Dubois for providing me with many of his unpublished DNS results on forced isotropic turbulence, to Dr. S. Otto for his unstinted help with regard to the computations, and to Dr. J. Hardin and Dr. C. Speziale for many helpful discussions and comments on an earlier version of this paper, but especially to Dr. S. Sarkar for his helpful discussions and comments throughout this study.

References

- Batchelor, G.K., 1951. "Pressure fluctuations in isotropic turbulence," *Proc. Cam. Phil. Soc.* **47** p.359.
- Batchelor, G.K., 1953. "The theory of homogeneous turbulence," *Cambridge University Press*.
- Comte-Bellot, G., and Corrsin, S., 1966. "The use of a contraction to improve the isotropy of a grid generated turbulence" , *J.Fluid Mech.* **25** pp. 657-682.
- Dubois, T., 1993. , *Private communication*. (Also see Debussche, A., Dubois, T., and Temam, R., 1993. "The nonlinear Galerkin method: A multi-scale method applied to the simulation of homogeneous turbulent flows." *ICASE Rep.93/93*.
- Herring, J.R., Riley, J.J., Patterson, G.S., and Kraichnan, R.H., 1973. "Growth of uncertainty in decaying isotropic turbulence" *J.Atm.Sc.* **91** p581.
- Hinze, J.O., 1975. "Turbulence," *McGraw Hill Inc* p.21 and p.59.
- Lesieur, M., 1990. "Turbulence in Fluids" *Kluwer Academic Publishers*.
- Lighthill, M.J., 1952. "On sound generated aerodynamically: 1. General theory," *Proc. Roy. Soc. (A)* **211**, p.1107.
- Lighthill, M.J., 1992. "An estimate of the covariance of T_{xx} without using statistical assumptions," see Appendix 1 of "On the noise radiated from a turbulent high speed jet," by Lilley, G.M. in "Computational aeroacoustics" by Hardin, J.C., and Hussaini, M.Y. *Springer Verlag*.
- Proudman, I., 1952. "The generation of noise by isotropic turbulence," *Proc. Roy. Soc. (A)* **214**, p.119 .
- Sarkar, S., and Hussaini, M.Y., 1993. "Computation of the sound generated by isotropic turbulence," *ICASE Rep.* **93-74**.
- Speziale, C.G., and Bernard, P.S., 1992. "The energy decay in isotropic turbulence revisited," *J. Fluid Mech.* **241**, p.645.
- Stewart, R.W., and Townsend, A.A., 1951. "Similarity and self-preservation in isotropic turbulence." *Phil. Trans. A.* **243**, p359.
- Townsend, A.A., 1956. "The structure of turbulent shear flow." *Cambridge University Press*.
- Warhaft, Z. and Lumley, J.L., 1978. "An experimental study of the decay of temperature fluctuations in grid generated turbulence," *J. Fluid Mech.* **88**, pp.659-684.
- Witkowska, A., and Juve, D., 1993. "Numerical simulations of the noise generated by homogeneous and isotropic turbulence." *Proc. 13th. Colloquium on Aero- and Hydroacoustics*.

Appendix 1

The length and time scales of isotropic turbulence

We will define the following length and velocity scales in isotropic turbulence. (i) Taylor microscale $= \lambda$, (ii) Kolmogoroff dissipation scale $= l_s$, (iii) Energy containing eddy (integral) scale $= L$, (iv) Velocity of Taylor microscale eddies $= u_\lambda$, (v) Velocity of Kolmogoroff eddies $= u_s$, (vi) Velocity of energy containing eddies $= \langle u^2 \rangle = u$.

Here $K = 3u^2/2 : \epsilon = 1.5u_s^3/l_s = 1.5u_\lambda^3/\lambda = 1.5u^3/L : f''(0) = -1/\lambda^2 : L = \int_0^\infty f(r)dr$. If ϵ is the kinematic dissipation function, then in isotropic turbulence,

$$\epsilon = 15\nu \frac{u^2}{\lambda^2} = 1.5 \frac{u^3}{L}, \quad (A1.1)$$

and so defining $R_L = uL/\nu$ as the flow Reynolds number based on the energy containing length scale and velocity, we find,

$$\frac{\lambda}{L} = \sqrt{\frac{10}{R_L}}, \quad (A1.2)$$

and if the Reynolds number of the microscale eddies is defined as $R_\lambda = u\lambda/\nu$ then,

$$R_\lambda = \sqrt{10}\sqrt{R_L}. \quad (A1.3)$$

During the decay both R_L and R_λ vary with time but in the initial period of decay both R_L and R_λ are constants. In this initial period of decay the kinetic energy of the turbulence, K is proportional to t^{-1} and both L and λ increase proportional to $t^{1/2}$. In the final period of decay both R_L and R_λ decrease with time with K falling as $t^{-5/2}$. But in this final period of decay we find although λ continues to increase as $t^{1/2}$ the energy containing scale L now falls as $t^{-1/4}$. Eventually R_L equals R_λ and this occurs when R_L equals 10, based on the defined quantities as given above. These results for the initial and final decay periods in isotropic self-preserving turbulence are tabulated in tables (1) and (2) below.

We also have the following relations. The Reynolds number of the Kolmogoroff eddies is unity, or,

$$\frac{u_s l_s}{\nu} = 1. \quad (A1.4)$$

The velocity flatness, $T_1 = \langle u^4 \rangle / \langle u^2 \rangle^2$, and the velocity skewness, $S_1 = \langle u^3 \rangle / \langle u^2 \rangle^{3/2}$, factors as measured by Townsend in isotropic turbulence have values close to 3, and zero respectively, which are the values when the joint probability distribution is normal. Further, from these same experiments, the velocity derivative flatness factor, $T_2 = \langle (\partial u / \partial x)^4 \rangle / \langle (\partial u / \partial x)^2 \rangle^2$, attains values nearer 4, and the velocity derivative skewness factor, $S_2 = \langle (\partial u / \partial x)^3 \rangle / \langle \partial u / \partial x \rangle^3$ becomes negative and attains values of the order of -0.5 . From Speziale and Bernard we note $S_2 = \lambda^3 k'''(0)$ and, $G = \lambda^4 f''''(0)$, where G is a function of the velocity derivative flatness factor. It is also given by $G = \frac{3\lambda^2}{7} \langle (\partial \omega_i / \partial x_j \partial \omega_i / \partial x_j) \rangle / \langle \omega_i \omega_i \rangle$. Here $k(r/L)$ is the scalar triple velocity correlation function, which is related to $f(r/L)$ through the Karman-Howarth equation.

In complete self-preserving isotropic turbulence both S_2 and G remain constant. For the stationary case, when $\langle u^2 \rangle$ is a constant, $R_\lambda = -2G/S_2$, and shows the large values of G , and hence of the flatness factors, that can occur at high values of the Reynolds number.

The relation between the scales L and l_s is,

$$\frac{L}{l_s} = R_L^{3/4}, \quad (A1.5)$$

and,

$$\frac{u}{u_s} = R_L^{1/4}. \quad (A1.6)$$

If we define the velocity corresponding to the Taylor microscale as u_λ then we find,

$$\frac{u_\lambda}{u} = \left(\frac{\lambda}{L}\right)^{1/3} = \frac{1.4678}{R_L^{1/6}}, \quad (A1.7)$$

since $\epsilon = 1.5u^3/L = 1.5u_\lambda^3/\lambda$. Similarly we find for the ratio of the characteristic frequencies of the Taylor microscale eddies, ω_λ , and the energy containing eddies, ω_L , respectively,

$$\frac{\omega_\lambda}{\omega_L} = 0.4642 R_L^{1/3}. \quad (A1.8)$$

We also find that for values of $R_L < 226$ and $R_\lambda < 48$ the peak frequency, ω_{max} , in the acoustic spectrum exceeds the frequency associated with the Taylor microscale eddies. The frequency of the Kolmogoroff eddies, ω_s , is related to the vorticity since, $\omega_s = u_s/l_s$, and the vorticity, ω , also has a magnitude of the order of u_s/l_s . As defined the Strouhal number of the Kolmogoroff eddies, $\omega_s l_s/u_s$, is unity. On the other hand the Strouhal number, s_L , of the energy containing eddies is equal to $\omega_L L/u$. (We can identify the Strouhal number, s_L , as equal to the turbulent Strouhal number, S_T , as used in the main text above.) We find using the relations above that,

$$S_T = s_L = \frac{\omega_L L}{u} = \frac{\omega_L}{\omega_s} R_L^{1/2}, \quad (A1.9)$$

and is a flow constant of order unity, which we assume here is equal to unity. Therefore $\omega_s/\omega_L = R_L^{1/2}$, and the peak frequency in the acoustic spectrum exceeds ω_s when $R_\lambda = 8.9$. These are essentially low Reynolds number limits and are approximate values only depending on the approximations made above with respect to the formulas for the dissipation function and the turbulent Strouhal number.

Other relations follow. The eddy turnover-time, a measure of the life-time of the dominant eddies, is $K/\epsilon = L/u = 1/\omega_L$, provided the turbulent Strouhal number, S_T , is of order unity, and is therefore proportional to the characteristic time of the energy containing eddies. Since $S_T = \Omega L/u = O(1)$, the characteristic time of the energy containing eddies is nearly $(\Omega)^{-1} = L/u = K/\epsilon$, the eddy turnover time. Similarly the characteristic time of the dissipating eddies is, $1/\omega_s = \sqrt{\nu/\epsilon}$. These results are tabulated in Table(3) for a large range of R_L . The values given for ω_{max} are equal to $\sqrt{8}\omega_L$.

Table 1.

Initial Decay.(Self-preserving flow.)

$u \sim t^{-1/2}$	$L \sim t^{1/2}$
$\epsilon \sim t^{-2}$	$\lambda \sim t^{1/2}$
$K \sim t^{-1}$	$\lambda \sim L$
$R_\lambda \sim R_L$	

Table 2.

Final Period of Decay.(Self-preserving flow.)

$u \sim t^{-5/4}$	$L \sim t^{-1/4}$
$\epsilon \sim t^{-7/2}$	$\lambda \sim t^{1/2}$
$K \sim t^{-5/2}$	$R_\lambda \sim t^{-3/4}$
$R_L \sim t^{-3/2}$	
$R_L = R_\lambda$ when $R_L = 10$	

Table 3.

Approximate Properties of Isotropic Turbulence.

R_L	R_λ	λ/L	l_s/λ	ω_{max}/ω_L	ω_λ/ω_L	ω_s/ω_λ	$\omega_{max}/\omega_\lambda$
10	10	1.0	0.1778	2.83	1.0	3.16	2.83
100	31.62	0.3162	0.1	2.83	2.15	4.64	1.31
1000	100	0.1	0.0562	2.83	4.64	6.81	0.61
10000	316.23	0.0316	0.0316	2.83	10.0	10.0	0.28
100000	1000	0.01	0.0178	2.83	21.54	14.68	0.13
1000000	3162.3	0.0032	0.01	2.83	46.42	21.54	0.06

Appendix 2

Derivation of Lighthill's Integral in Homogeneous Turbulence.

Lighthill(1952) showed that the density fluctuation at a far-field observer at \mathbf{x} at time t due to a quadrupole distribution of T_{xx} per unit volume at a source positions \mathbf{y} at the source, or retarded, time τ , is given by

$$(\rho(\mathbf{x}, t) - \rho_\infty) = \frac{1}{4\pi x c_\infty^4} \int d\mathbf{y} \frac{\partial^2 T_{xx}}{\partial \tau_A^2}(\mathbf{y}, \tau_A), \quad (A2.1)$$

where $\tau_A = t - |\mathbf{x} - \mathbf{y}|/c_\infty$. If we next find the similar expression for the density fluctuation at \mathbf{x} from a source position \mathbf{z} and at an observer time of $t + t^*$ then

$$(\rho(\mathbf{x}, t) - \rho_\infty)(\rho(\mathbf{x}, t + t^*) - \rho_\infty)$$

$$= \frac{1}{16\pi^2 x^2 c_\infty^8} \int d\mathbf{y} \int d\mathbf{z} \frac{\partial^2 T_{xx}}{\partial \tau_A^2}(\mathbf{y}, \tau_A) \frac{\partial^2 T_{xx}}{\partial \tau_B^2}(\mathbf{z}, \tau_B), \quad (\text{A2.2})$$

where $\tau_B = t + t^* - |\mathbf{x} - \mathbf{z}|/c_\infty$. If the turbulence is homogeneous in space at any given time, t_d , during the decay from some given initial state, then by defining $t = t_d + t'$, $\tau = \tau_B - \tau_A$, $\tau_s = (\tau_A + \tau_B)/2$, $\mathbf{r} = \mathbf{z} - \mathbf{y}$, we find

$$\tau_s = t_d - x/c_\infty, \quad (\text{A2.3})$$

and noting τ_A is a function of both t_d and t'

$$\begin{aligned} & (\rho(\mathbf{x}, t_d + t') - \rho_\infty)(\rho(\mathbf{x}, t_d + t' + t^*) - \rho_\infty) \\ &= \frac{1}{16\pi^2 x^2 c_\infty^8} \int d\mathbf{y} \int d\mathbf{r} \frac{\partial^4}{\partial \tau_A^2 \partial \tau_B^2} T_{xx}(\mathbf{y}, \tau_A) T_{xx}(\mathbf{y} + \mathbf{r}, \tau_A + \tau). \end{aligned} \quad (\text{A2.4})$$

Since ρ and T_{xx} are random functions of time we can find their means, or average values at any given time, t_d , during the decay, by either integrating with respect to t' over a sufficient time around t_d , or finding the equivalent volume integral, at the given time for each value of the separation distance \mathbf{r} . For homogeneous turbulence the volume integration will be over all \mathbf{y}' , surrounding the fixed point \mathbf{y} , of

$$\frac{\partial^2}{\partial \tau_A^2} T_{xx}(\mathbf{y} + \mathbf{y}', \tau_A) \frac{\partial^2}{\partial \tau_B^2} T_{xx}(\mathbf{y} + \mathbf{y}' + \mathbf{r}, \tau_B). \quad (\text{A2.5})$$

Hence the autocorrelation of the acoustic power per unit volume of turbulence at time t_d and time separation t^* is

$$p_s(t_d, t^*) = \frac{\rho_\infty}{4\pi c_\infty^5} \int U(t_s, \mathbf{r}, \tau) d\mathbf{r}, \quad (\text{A2.6})$$

where

$$U(t_s, \mathbf{r}, \tau) = \left\langle \frac{\partial^4}{\partial \tau_A^2 \partial \tau_B^2} T_{xx}(\mathbf{y}, \tau_A) T_{xx}(\mathbf{y} + \mathbf{r}, \tau_A + \tau) \right\rangle, \quad (\text{A2.7})$$

and t_s is related to t_d by Equation(A1.3) and t^* to τ and \mathbf{r} . Here we have assumed that T_{xx} may be approximated by $T_{xx} = u_x^2$. Since taking the average and differentiating with respect to τ_A and τ_B permute we find

$$U(t_s, \mathbf{r}, \tau) = \frac{\partial^2}{\partial \tau_A^2 \partial \tau_B^2} \langle u_x^2(\mathbf{y}, \tau_A) u_x^2(\mathbf{z}, \tau_B) \rangle, \quad (\text{A2.8})$$

where $\langle \rangle$ denotes the average value, or ensemble average at the source time, t_s , corresponding to time, t_d , at the observer. The assumption is also made here that the random fluctuations in the turbulence, on average, have a continuous spectrum and similarly with respect to the far field acoustic power spectrum. Thus we can find the power spectral density at the decay time t_d giving

$$p_s(t_d, \omega) = \frac{\rho_\infty}{4\pi c_\infty^5} \int d\mathbf{r} \exp(-i\mathbf{k} \cdot \mathbf{r}) \int d\tau \exp(-i\omega\tau) \frac{\partial^4}{\partial \tau_A^2 \partial \tau_B^2} P_{xx,xx}(t_s, \mathbf{r}, \tau), \quad (\text{A2.9})$$

where $P_{xx,xx}$ is the covariance of u_x^2 , at time, t_s , and $\mathbf{k} = -\omega \mathbf{x} / x c_\infty$ is the wave number vector in the turbulence in the direction of the propagation to the distant observer. Its amplitude in our near incompressible flow is almost zero. The time differentiations with respect to τ_A and τ_B can be replaced by differentiations with respect to τ and t_s and the operator

$$\frac{\partial^4}{\partial \tau_A^2 \partial \tau_B^2} \equiv \left(\frac{\partial^2}{\partial \tau^2} - \frac{\partial^2}{4\partial t^2} \right)^2 = \frac{\partial^4}{\partial \tau^4} - \frac{1}{2} \frac{\partial^4}{\partial t^2 \partial \tau^2} + \frac{1}{16} \frac{\partial^4}{\partial t^4}. \quad (\text{A2.10})$$

In general the operator is dominated by the differentiations with respect to τ . We find from the known time dependence of the fall in the turbulent kinetic energy during the decay that the ratio of the terms is of order (1 : 0.02 : 0.0003). In the earlier work of Proudman(1952) similar ratios were found. Thus we can write to a good approximation

$$p_s(t_d, \omega) = \frac{\omega^4 \rho_\infty}{4\pi c_\infty^5} \int d\mathbf{r} \exp(-i\mathbf{k} \cdot \mathbf{r}) P_{xx,xx}(t_s, \mathbf{r}, \omega), \quad (\text{A2.11})$$

which is the expression used in Section(3) above.

Appendix 3

Proudman's Evaluation of the Lighthill Integral

In the notation of Section(2) above we found the equivalent acoustic source scalar function U (see Equation(2.6))

$$U = 8S_{AB}^2 + 4R_{AB}T_{AB} + 4V_1 + 8(V_2 + V_3), \quad (\text{A3.1})$$

and using the values for R_{AB} , S_{AB} , V_1 , V_2 , and V_3 given in Equation(2.7) we find

$$U = 8\left(\frac{\partial^2 R_{AB}}{\partial t_A \partial t_B}\right)^2 + 4R_{AB} \frac{\partial^4 R_{AB}}{\partial t_A^2 \partial t_B^2} + 4 \frac{\partial^2 R_{AB}}{\partial t_A^2} \frac{\partial^2 R_{AB}}{\partial t_B^2} + 8\left(\frac{\partial R_{AB}}{\partial t_A} \frac{\partial^3 R_{AB}}{\partial t_A \partial t_B^2} + \frac{\partial R_{AB}}{\partial t_B} \frac{\partial^3 R_{AB}}{\partial t_B \partial t_A^2}\right). \quad (\text{A3.2})$$

If we introduce the notation:

$$t = \frac{t_A + t_B}{2} : \tau = t_B - t_A, \quad (\text{A3.3})$$

where t is the mean source time and τ is the retarded time separation or difference. We need the following transformation formulae in order to transform our basic equations in τ_A and τ_B into equations in t and τ . These are:

$$\frac{\partial}{\partial t_A} = \frac{\partial}{\partial t} \frac{\partial t}{\partial \tau_A} + \frac{\partial}{\partial \tau} \frac{\partial \tau}{\partial \tau_A} = \frac{\partial}{\partial t} - \frac{\partial}{\partial \tau}. \quad (\text{A3.4})$$

$$\frac{\partial}{\partial t_B} = \frac{\partial}{\partial t} \frac{\partial t}{\partial \tau_B} + \frac{\partial}{\partial \tau} \frac{\partial \tau}{\partial \tau_B} = \frac{\partial}{\partial t} + \frac{\partial}{\partial \tau}. \quad (\text{A3.5})$$

$$\frac{\partial^2}{\partial t_A^2} = \frac{\partial^2}{\partial t^2} - \frac{\partial^2}{\partial t \partial \tau} + \frac{\partial^2}{\partial \tau^2}. \quad (\text{A3.6})$$

$$\frac{\partial^2}{\partial t_B^2} = \frac{\partial^2}{\partial t^2} + \frac{\partial^2}{\partial t \partial \tau} + \frac{\partial^2}{\partial \tau^2}. \quad (\text{A3.7})$$

It follows that,

$$S_{AB} = \frac{\partial^2 R_{AB}}{\partial t^2} - \frac{\partial^2 R_{AB}}{\partial \tau^2}. \quad (\text{A3.8})$$

$$\frac{\partial^4 R_{AB}}{\partial t_A^2 \partial t_B^2} = \frac{\partial^2 S_{AB}}{\partial \tau_A \partial \tau_B} = \frac{\partial^4 R_{AB}}{16 \partial t^4} - \frac{\partial^4 R_{AB}}{2 \partial t^2 \partial \tau^2} + \frac{\partial^4 R_{AB}}{\partial \tau^4}. \quad (\text{A3.9})$$

$$\begin{aligned} \frac{\partial^2 R_{AB}}{\partial t_A^2} \frac{\partial^2 R_{AB}}{\partial t_B^2} &= \left(\frac{\partial^2 R_{AB}}{4 \partial t^2} \right)^2 + \frac{2 \partial^2 R_{AB}}{4 \partial t^2} \frac{\partial^2 R_{AB}}{\partial \tau^2} - \left(\frac{\partial^2 R_{AB}}{\partial t \partial \tau} \right)^2 + \\ &\quad \left(\frac{\partial^2 R_{AB}}{\partial \tau^2} \right)^2. \end{aligned} \quad (\text{A3.10})$$

$$\frac{\partial R_{AB}}{\partial t_A} + \frac{\partial R_{AB}}{\partial t_B} = \frac{\partial R_{AB}}{\partial t}. \quad (\text{A3.11})$$

$$\frac{\partial R_{AB}}{\partial t_A} \frac{\partial^3 R_{AB}}{\partial t_A \partial t_B^2} + \frac{\partial R_{AB}}{\partial t_B} \frac{\partial^3 R_{AB}}{\partial t_B \partial t_A^2} =$$

$$\frac{\partial R_{AB}}{8 \partial t} \frac{\partial^3 R_{AB}}{\partial t^3} - \frac{\partial R_{AB}}{2 \partial \tau} \frac{\partial^3 R_{AB}}{\partial t^2 \partial \tau} - \frac{\partial R_{AB}}{2 \partial t} \frac{\partial^3 R_{AB}}{\partial t \partial \tau^2} + 2 \frac{\partial R_{AB}}{\partial \tau} \frac{\partial^3 R_{AB}}{\partial \tau^3}. \quad (\text{A3.12})$$

The further reduction using Equations (A3.4) to (A3.12) gives, if we write here $R = R_{AB} = \langle uu' \rangle$,

$$U = 12R_{\tau\tau}^2 + 4RR_{\tau\tau\tau\tau} + 16R_{\tau}R_{\tau\tau\tau}$$

$$\frac{3}{4}R_{tt}^2 + \frac{1}{4}RR_{tttt} - 4R_{t\tau}^2 - 2R_{tt}R_{\tau\tau} - 2RR_{tt\tau\tau} + R_tR_{ttt} - 4R_{\tau}R_{tt\tau} - 4R_tR_{t\tau\tau}, \quad (A3.13)$$

where all the terms involving derivatives with respect to t vanish when the flow is stationary. In the stationary flow case we find as given in equation(11)

$$U = 12R''^2 + 16R'R''' + 4RR'''' \quad (A3.14)$$

where the primes denote differentiating with respect to τ . Equations (A3.13) and (A3.14) are the main equations derived in this present analysis. In particular Equation(A3.13) has been derived with all effects of retarded time retained.

In Proudman(1952) Lighthill's fourth-order covariance is evaluated for the case of near incompressible isotropic turbulence or low Mach numbers, which is exactly the case we have considered above. In this limit the effect of retarded-time differences between the separated points A and B is small and is neglected by Proudman. According to Proudman's approximation $t_A = t_B$. Using Proudman's notation, and as published,

$$U = 12 \langle u_t u'_t \rangle^2 + 4 \langle uu' \rangle \langle u_{tt} u'_{tt} \rangle + 4 \langle (uu')_t \rangle \langle (u_t u'_t)_t \rangle +$$

$$\langle (uu')_{tt}^2 \rangle - 4 \langle (uu')_{tt} \rangle \langle u_t u'_t \rangle, \quad (A3.15)$$

where here t is equal to our t_A . When we compare Equation(A3.15) with our Equation(2.5) above, we note large differences between them, and yet both equations have been derived from Equation(2.3). In our notation, but putting $t_A = t_B$, Proudman's Equation as given by (A3.15) may be rewritten,

$$U = 9R''^2 + 4RR'''' + 4R'R''', \quad (A3.16)$$

where primes denote differentiating with respect to $t = t_A$, and differs from Equation(3.14) as derived in our revised analysis.

The differences arise, as we will show below, in that Proudman has put the retarded time difference to zero before evaluating the time differentials, and hence the complete evaluation of the Lighthill Integral is based on simultaneous covariances.

As stated above Proudman neglects the retarded time difference between the velocities and their time derivatives at the separated points A and B and hence sets $t_A = t_B$ throughout his analysis. Thus we can find U by following the above analysis leading to Equation(2.6), and then introducing the assumption $t_A = t_B$. (The further reduction as performed by Proudman is simplified, if we define $t \equiv t_A$.) If we now also introduce the isotropy condition that,

$$\langle uu'_t \rangle = \langle u'u_t \rangle, \quad (\text{A3.17})$$

then derivatives at A and B become simultaneous derivatives.

(In our treatment, with the retarded-time differences retained, we find,

$$\langle uu'_{t_B} \rangle \neq \langle u'u_{t_A} \rangle,$$

since,

$$\langle uu'_{t_B} \rangle = \frac{\partial R_{AB}}{\partial t_B},$$

$$\langle u'u_{t_A} \rangle = \frac{\partial R_{AB}}{\partial t_A},$$

and from Equations (A3.4) and (A3.5) we see these are not equal.)

However the result given by Equation (A3.17) is true in the case of simultaneous covariances and then we find,

$$4 \langle uu'_{tt} \rangle \langle u'u_{tt} \rangle = \left(\frac{\partial^2 \langle uu' \rangle}{\partial t^2} \right)^2 + 4 \langle u'_t u_t^2 \rangle - 4 \langle u'_t u_t \rangle \frac{\partial^2 \langle uu' \rangle}{\partial t^2}, \quad (\text{A3.18})$$

and,

$$8(\langle uu'_t \rangle \langle u'_t u'_{tt} \rangle + \langle u'u_t \rangle \langle u_t u'_{tt} \rangle) = 4 \frac{\partial \langle uu' \rangle}{\partial t} \frac{\partial \langle u'_t u_t \rangle}{\partial t}. \quad (\text{A3.19})$$

With these two results substituted into Equation (2.5) we find that Equation (2.5) reduces to Proudman's result given in Equation (A3.16) above.

Thus we see that Proudman's result is correct on the basis of the assumptions made regarding (i) isotropy, (ii) joint normal probability distribution, and (iii) simultaneous space covariances, when the latter assumption is made at the commencement of the analysis. The result is that Proudman's assumptions lead to extra terms in U . The correct result is only obtained when the simultaneous covariance assumption is included at the end of the analysis. In our work we replace Proudman's Equation (A3.16) by our Equation (A3.14), which was given as Equation (2.8) above.

With the assumption of simultaneous covariances Proudman finds all the two-point covariances in terms of the longitudinal correlation coefficient $f(r, t)$ where r is the space separation and t denotes the time during the decay of the isotropic turbulence.

The evaluation of the various two-point second order covariances in U in our work can also be evaluated by use of the same derivation as found from Proudman's paper for the case where the retarded time differences are neglected, and it is this approximation we now introduce. Proudman shows that U depends only on three second order tensors which finally are shown to be functions of a single scalar function, $f(r)$, the longitudinal velocity correlation function. These second order tensors, which are all solenoidal, are,

$$\langle u_i u'_j \rangle = \langle u^2 \rangle \left[-\frac{1}{2r} f' r_i r_j + \left(\frac{1}{2} r f' + f \right) \delta_{ij} \right], \quad (\text{A3.20})$$

$$\left\langle \frac{\partial u_i}{\partial t} \frac{\partial u'_j}{\partial t} \right\rangle = \left\langle \left(\frac{\partial u}{\partial t} \right)^2 \right\rangle \left[-\frac{1}{2r} \phi' r_i r_j + \left(\frac{1}{2} r \phi' + \phi \right) \delta_{ij} \right], \quad (\text{A3.21})$$

$$\left\langle \frac{\partial^2 u_i}{\partial t^2} \frac{\partial^2 u'_j}{\partial t^2} \right\rangle = \left\langle \left(\frac{\partial^2 u}{\partial t^2} \right)^2 \right\rangle \left[-\frac{1}{2r} \psi' r_i r_j + \left(\frac{1}{2} r \psi' + \psi \right) \delta_{ij} \right], \quad (\text{A3.22})$$

where f, ϕ, ψ are even scalar functions of r and dashes denote differentiation with respect to r . We note u is differentiated with respect to time t_A and u' is differentiated with respect to time t_B with the ensemble averages evaluated at $t_A = t_B$, and the retarded time difference is then put equal to zero. Thus although the covariances R and its derivatives in Equation (A3.13) are functions of \mathbf{r}, t, τ they are reduced in this low Mach number approximation to functions of (\mathbf{r}, t) only. When the flow locally at any time during the decay is assumed to be stationary we see that the covariance R and its derivatives are taken with respect to τ only and then evaluated at time τ equal to zero. It is these values of R that Proudman finds can be evaluated from the Euler equations of motion, in terms of equivalent space covariances, since at high Reynolds numbers the effects of viscosity can be ignored.

In the special case of stationary flow we find,

$$\begin{aligned} \iiint U d\mathbf{r} &= \frac{8\pi}{15} \int_0^\infty r^4 dr \left(12 \left\langle \left(\frac{\partial u}{\partial t} \right)^2 \right\rangle^2 \phi'^2 + \right. \\ &\quad \left. 4 \langle u^2 \rangle \left\langle \left(\frac{\partial^2 u}{\partial t^2} \right)^2 \right\rangle f' \psi' + 16 \frac{\partial}{\partial t} \left(\langle u^2 \rangle f' \right) \frac{\partial}{\partial t} \left(\left\langle \left(\frac{\partial u}{\partial t} \right)^2 \right\rangle \phi' \right) \right). \end{aligned} \quad (\text{A3.23})$$

The simplified forms of the solenoidal tensors in Equation (A3.23) arises from their volume integration and noting that its integrand involves only components of the velocity aligned in the direction between source and observer. In addition we note that,

$$\int_0^{2\pi} d\phi \int_0^\pi \sin^5 \theta d\theta \int_0^\infty \frac{1}{4} r^4 \phi'^2 dr = \frac{8\pi}{15} \int_0^\infty r^4 \phi'^2 dr, \quad (\text{A3.24})$$

and similarly for the tensors involving f and ψ . From Proudman we find, taking the trace of $\left\langle \frac{\partial u_i}{\partial t} \frac{\partial u'_i}{\partial t} \right\rangle$,

$$\left\langle \frac{\partial u_i}{\partial t} \frac{\partial u'_i}{\partial t} \right\rangle = \left\langle \left(\frac{\partial u}{\partial t} \right)^2 \right\rangle > \frac{1}{r^2} \frac{d}{dr} (r^3 \phi), \quad (\text{A3.25})$$

and using the Euler equations together with the assumption of a normal joint velocity distribution,

$$\left\langle \frac{\partial u_i}{\partial t} \frac{\partial u'_i}{\partial t} \right\rangle = \frac{1}{\rho_\infty^2} \nabla^2 \langle pp' \rangle - \frac{\partial^2}{\partial r_j \partial r_k} \langle u_i u_j u'_i u'_k \rangle, \quad (\text{A3.26})$$

with,

$$\frac{\partial^2}{\partial r_j \partial r_k} \langle u_i u_j u'_i u'_k \rangle = (\langle u^2 \rangle)^2 \frac{1}{r^2} \frac{d}{dr} [r^3 (f f'' - \frac{1}{2} f'^2 + \frac{4}{r} f f')] \quad (\text{A3.27}),$$

giving,

$$\langle (\frac{\partial u}{\partial t})^2 \rangle \phi = \frac{1}{\rho_\infty^2} \frac{1}{r} \frac{d}{dr} \langle p p' \rangle - (\langle u^2 \rangle)^2 (f f'' - \frac{1}{2} f'^2 + \frac{4}{r} f f') \quad (\text{A3.28})$$

and,

$$\frac{1}{\rho_\infty^2} \langle p p' \rangle = 2 (\langle u^2 \rangle)^2 \int_r^\infty (\eta - \frac{r^2}{\eta}) f'^2 d\eta. \quad (\text{A3.29}).$$

Also,

$$\langle \frac{\partial^2 u_i}{\partial t^2} \frac{\partial^2 u'_i}{\partial t^2} \rangle = \frac{1}{\rho_\infty^2} \nabla^2 \langle \frac{\partial p}{\partial t} \frac{\partial p'}{\partial t} \rangle - \frac{\partial^2}{\partial r_j \partial r_k} \langle \frac{\partial u_i u_j}{\partial t} \frac{\partial u'_i u'_k}{\partial t} \rangle \quad (\text{A3.30})$$

and,

$$\begin{aligned} \langle (\frac{\partial u}{\partial t})^2 \rangle \psi &= \frac{1}{\rho_\infty^2} \frac{d}{r dr} \langle \frac{\partial p}{\partial t} \frac{\partial p'}{\partial t} \rangle - \\ &\langle u^2 \rangle \langle (\frac{\partial u}{\partial t})^2 \rangle (-3 f' \phi' + \frac{d^2(f \phi)}{dr^2} + \frac{4}{r} \frac{d(f \phi)}{dr}) \end{aligned} \quad (\text{A3.31})$$

where,

$$\frac{1}{\rho_\infty^2} \langle \frac{\partial p}{\partial t} \frac{\partial p'}{\partial t} \rangle = 4 \langle u^2 \rangle \langle (\frac{\partial u}{\partial t})^2 \rangle \int_r^\infty (\eta^2 - r^2) f' \phi' \frac{d\eta}{\eta} \quad (\text{A3.32})$$

and,

$$\langle (\frac{\partial u}{\partial t})^2 \rangle \psi' = - \langle u^2 \rangle \langle (\frac{\partial u}{\partial t})^2 \rangle [\phi(f'''' + \frac{4f''}{r} - \frac{4f'}{r^2}) + f(\phi'''' + \frac{4\phi''}{r} - \frac{4\phi'}{r^2})]. \quad (\text{A3.33})$$

If we follow Proudman's notation then for the case of stationary flow we write,

$$p_s = \frac{\alpha \rho_\infty u^8}{c_\infty^5 L}, \quad (\text{A3.34})$$

and using the formulae above, and substituting into Equation(A3.23), we find α is equal to,

$$\alpha = \frac{8}{5} \int_0^\infty f^2 G^2 x^4 dx,$$

$$\begin{aligned}
& -\frac{8}{15} \int_0^\infty f' \left[G \int_x^\infty f G dx + f \left(\frac{4}{x^2} f G - \frac{4}{x} \frac{d}{dx} (f G) - \frac{d^2}{dx^2} (f G) \right) \right] x^4 dx \\
& + \frac{32}{135} \int_0^\infty (3f' + x f'')(7fG + x \frac{d}{dx} (fG)) x^4 dx,
\end{aligned} \tag{A3.35}$$

and

$$G = f''' + \frac{4}{x} f'' - \frac{4}{x^2} f'. \tag{A3.36}$$

This expression for α differs from that given by Proudman(1952) due to the differences in the contributions to the function U , as given in Equation(A3.16). The reasons for these differences are discussed fully above. When we substitute $\exp(-r^2/l^2)$ for $f(r/l)$ we find $\alpha = 12.36$ compared with the value of $\alpha = 13.5$ given by Proudman for $f(r/L) = \exp(-\pi r^2/4L^2)$. When we put $L = l\sqrt{\pi}/2$ in our result we find

$$p_s = \frac{10.96 \rho_\infty u^8}{L c_\infty^5}. \tag{A3.37}$$

For any given scalar longitudinal velocity distribution function, $f(r/L)$ the values of U and α can be found from Equations (A3.14) and (A3.35) with (A3.36) respectively.

For the non-stationary case U must be evaluated from Equation (A3.13) for the prescribed decay law for $\langle u^2 \rangle$ as a function of time. This generates additional terms in α , which, following Proudman's results, we may assume are very small compared with those given in Equation (A3.35), except in the immediate vicinity of the commencement of the decay before the self-preserving domain has been established. As Proudman states, the theory, as described here, does not apply to this region, and hence for most practical purposes the dominant sound power generated by a field of isotropic turbulence is that due to the sound generated at any time during the decay as if locally it were a stationary process. Hence it is independent very nearly of the decay law for the kinetic energy.

Appendix 4

Derivation of the Time-Dependent Fourth-Order Covariance in a Homogeneous Flow.

We write:

$$P(\mathbf{y}, t : \mathbf{r}, \tau) = \frac{< (T_{xx} - < T_{xx} >) (T'_{xx} - < T'_{xx} >) >}{< T_{xx} >^2}, \quad (A4.1)$$

where P is the noise source correlation function, and we have made the assumption that $< T_{xx} >$ is equal to $< T'_{xx} >$. Here T_{xx} is the aligned component of T_{ij} in the direction between the source and the distant observer, and the constant density term has been removed. P involves the fourth order covariance between the flow properties at two separated points in space and time.

Now the acoustic power output from isotropic turbulence per unit volume in near incompressible flow at low Mach numbers is,

$$p_s(\mathbf{x}, t : t^*) = \frac{\rho_\infty}{4\pi c_\infty^5} \iiint d\mathbf{r} \frac{\partial^4}{\partial t_A^2 \partial t_B^2} (P(\mathbf{y}, t : \mathbf{r}, \tau) < T_{xx} >^2), \quad (A4.2)$$

and using the results of Appendix 3. we find the fourth-time derivative of $< T_{xx} >^2 P(\dots, \tau)$ is:

$$< T_{xx} >^2 P'''' - \frac{d< T_{xx} >^2}{2dt^2} P'' + \frac{d^4< T_{xx} >^2}{16dt^4} P. \quad (A4.3)$$

At low Mach numbers the frequency, γ , of noise at the observer, is equal to the frequency, ω , of noise at the source, and then for the case of stationary flow:

$$p_s(\mathbf{x}, t : \omega) = \frac{2\pi^2 \rho_\infty}{c_\infty^5} \iiint \frac{d\mathbf{r}}{2\pi^3} \int \frac{d\tau}{2\pi} \exp(-i\omega\tau) \exp(-i\mathbf{k} \cdot \mathbf{r}) < T_{xx} >^2 \frac{\partial^4}{\partial \tau^4} P. \quad (A4.4)$$

If $P(\mathbf{r}, \tau)$ is a symmetric function of both \mathbf{r} and τ then the terms in odd powers of ω are zero. Thus we find,

$$p_s(\omega) = \frac{2\pi^2 \rho_\infty < T_{xx} >^2}{c_\infty^5} \omega^4 P(\mathbf{k}, \omega), \quad (A4.5)$$

where $< T_{xx} >^2$ is evaluated at time, t . This expression for the power spectral density is used in Section(3) above.

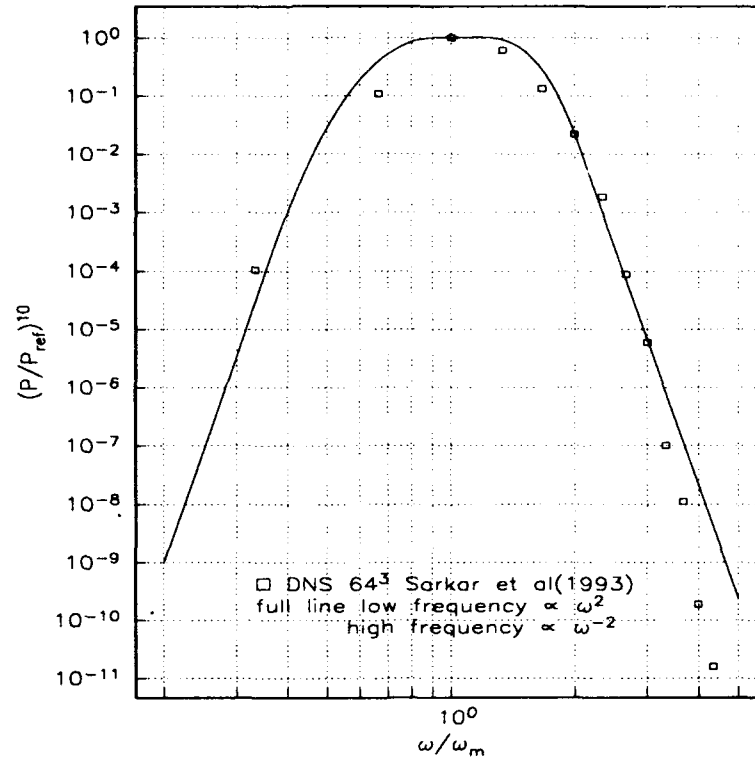


Figure 1: The Acoustic Energy Spectrum.

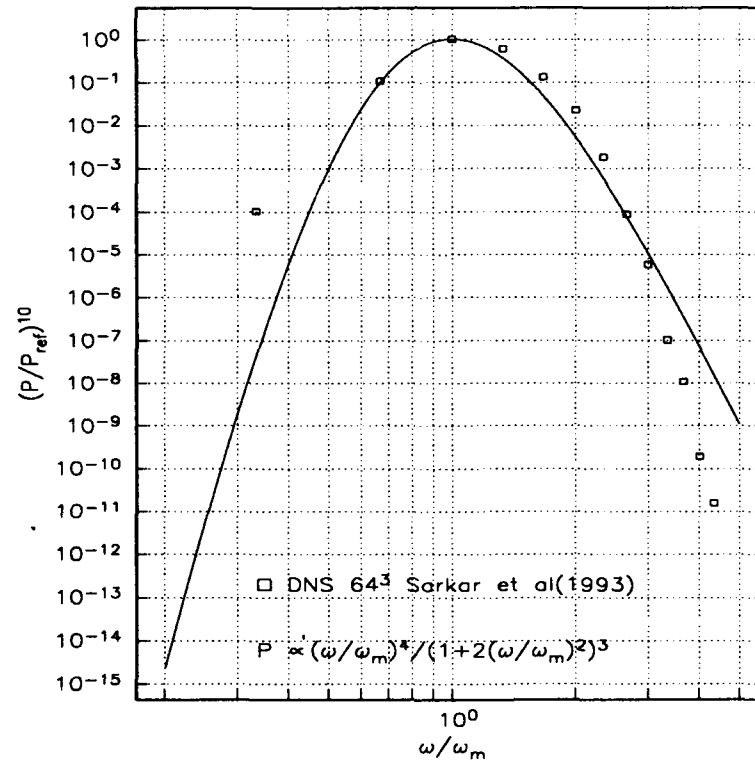


Figure 2: The Acoustic Energy Spectrum.

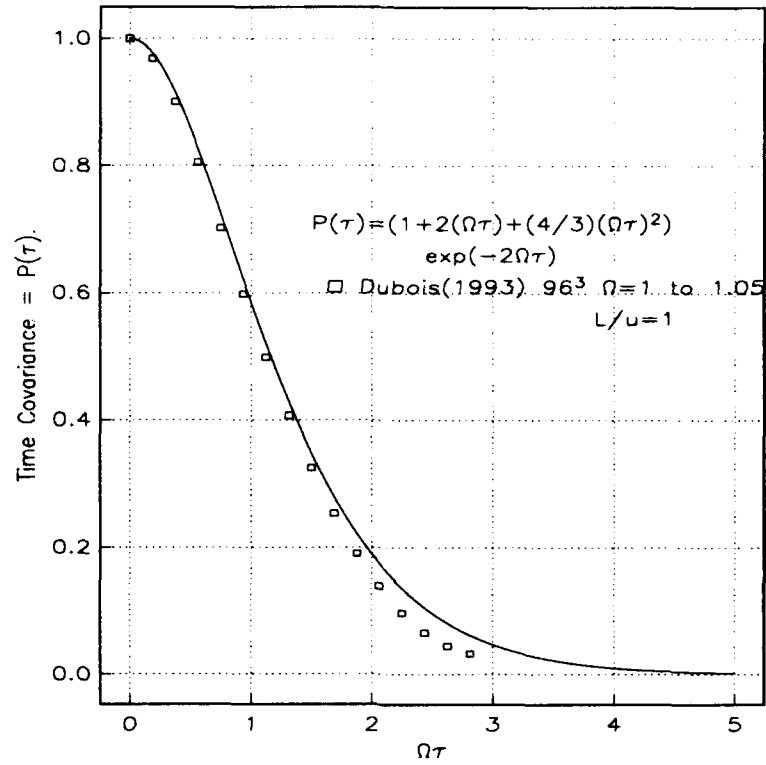


Figure 3: Temporal Acoustic Source Covariance.

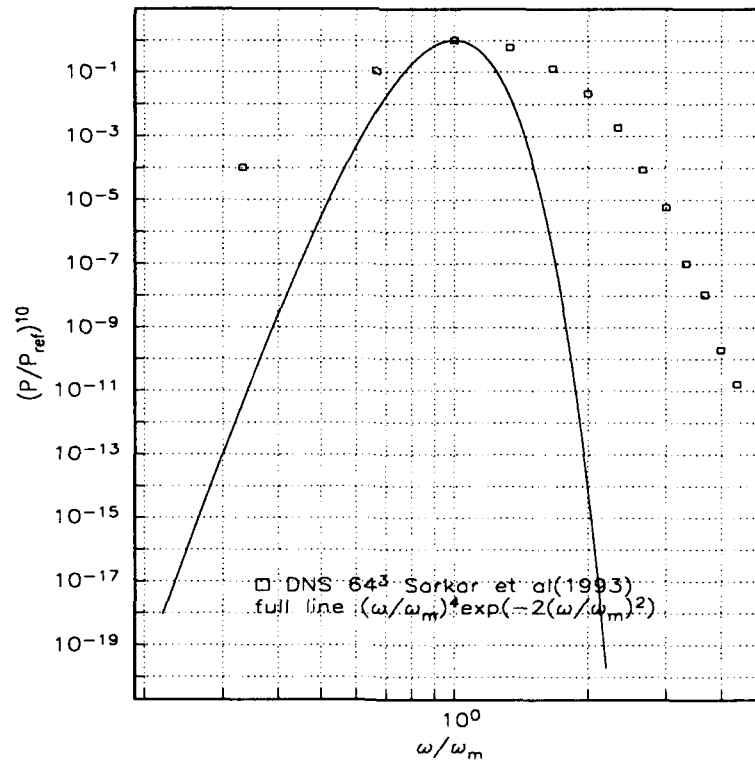


Figure 4: Acoustic Energy Spectrum.

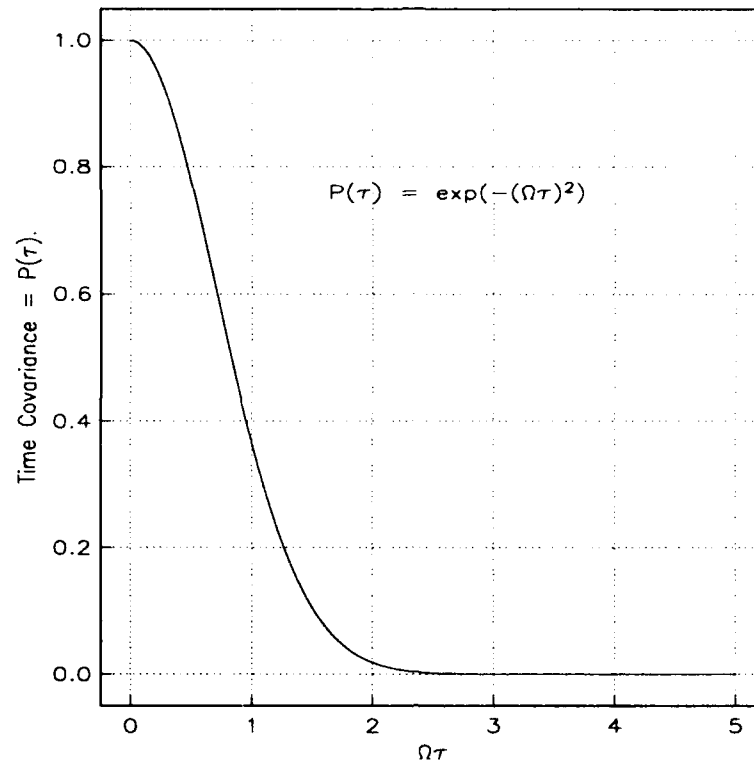


Figure 5: Temporal Acoustic Source Covariance.

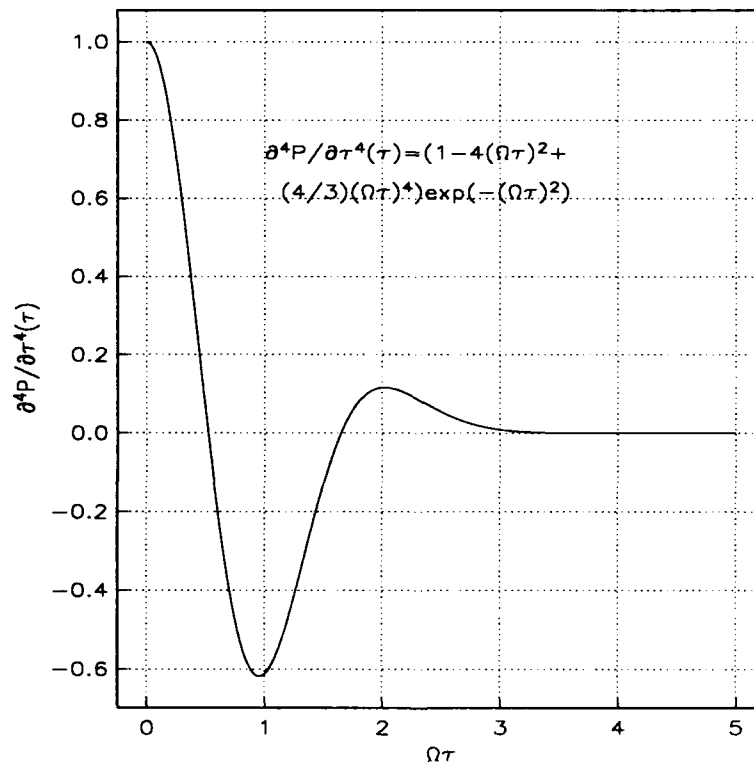


Figure 6: The Fourth Time Derivative of the Acoustic Source Covariance.

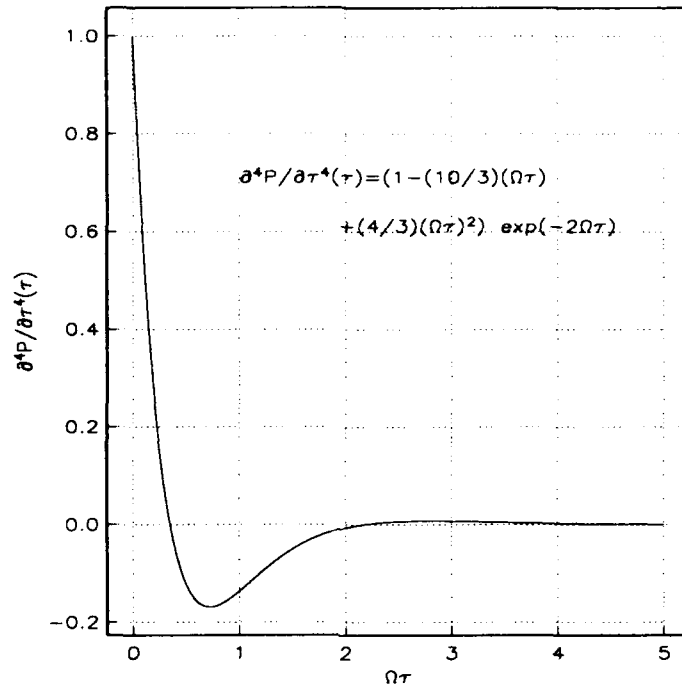


Figure 7: The Fourth Time Derivative of the Acoustic Source Covariance.

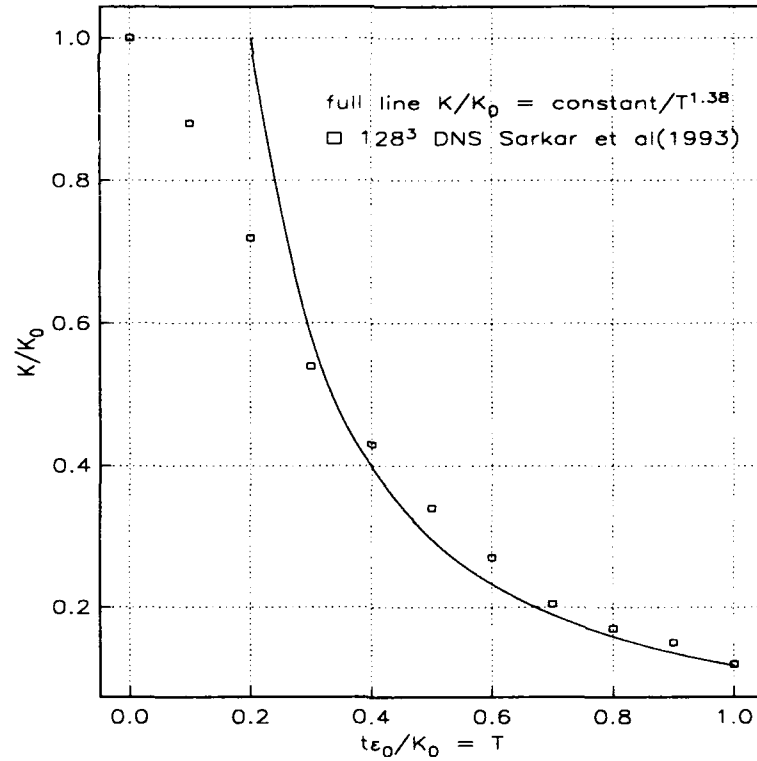


Figure 8: Decay of Kinetic Energy $K(T)$.

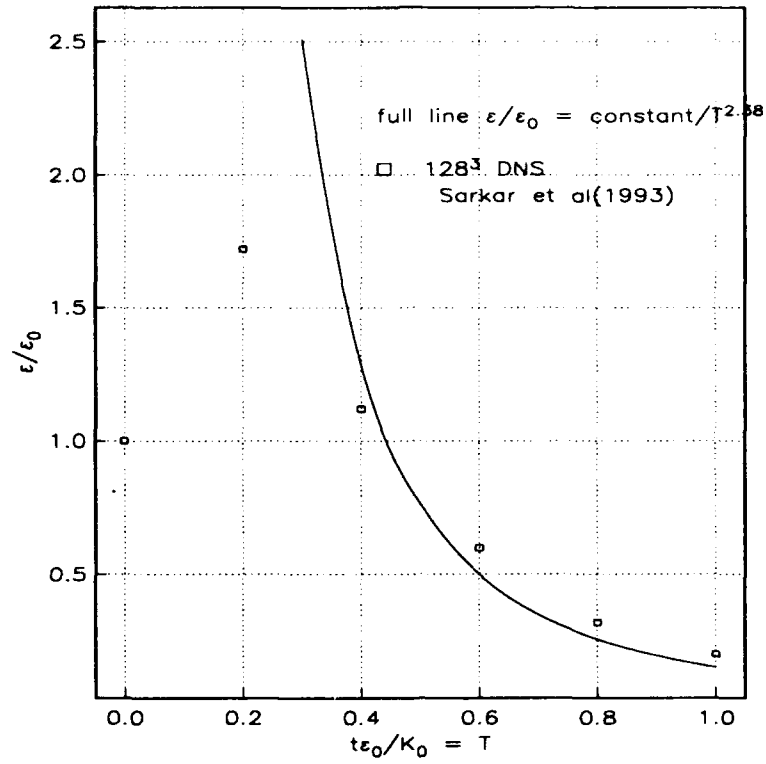


Figure 9: Decay of Dissipation Rate Function $\epsilon(T)$.

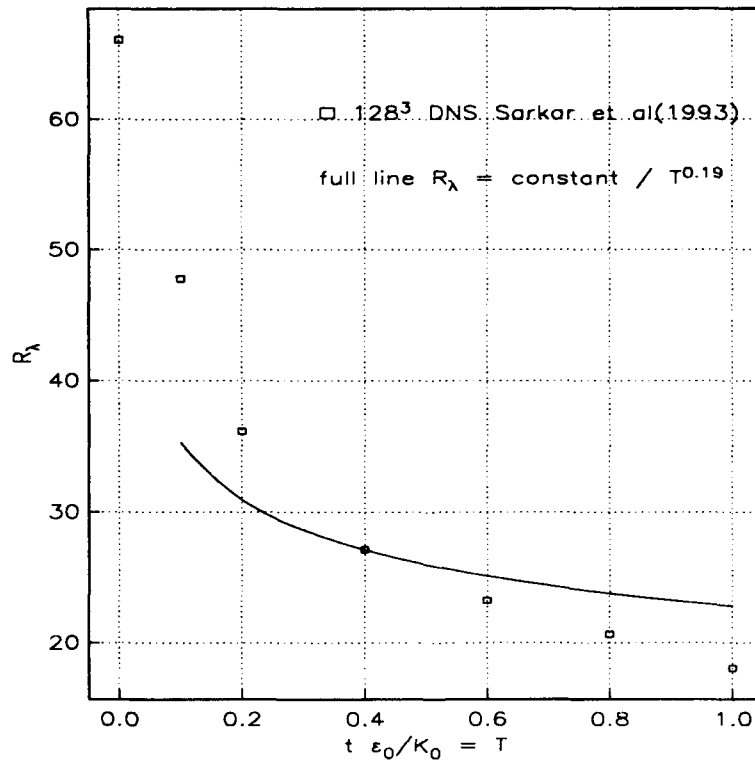


Figure 10: Variation of Taylor microscale Reynolds number R_λ .

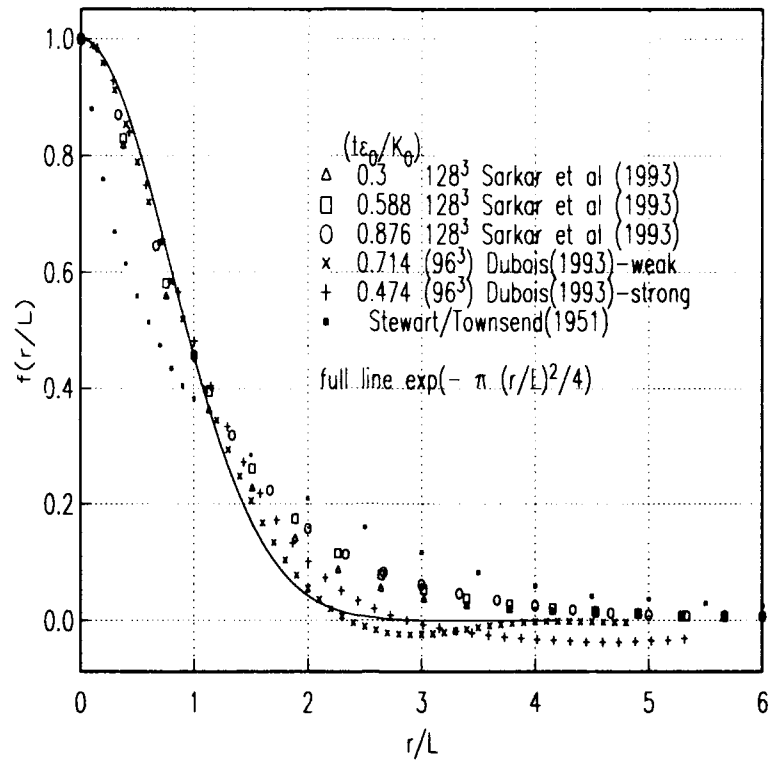


Figure 11: Longitudinal Velocity Correlation Function.

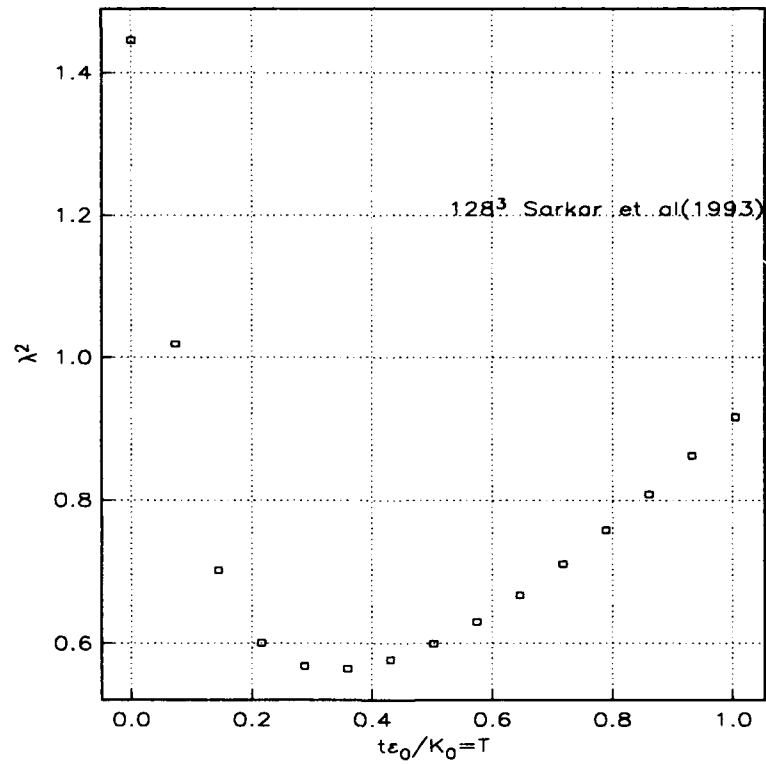


Figure 12: Variation of the square of Taylor microscale.

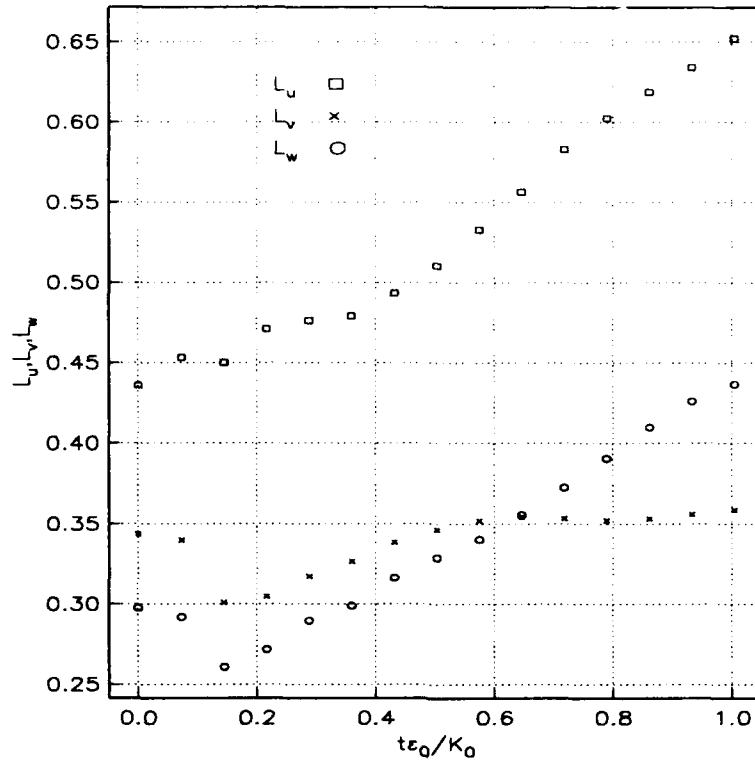


Figure 13: Variation of Integral scales.

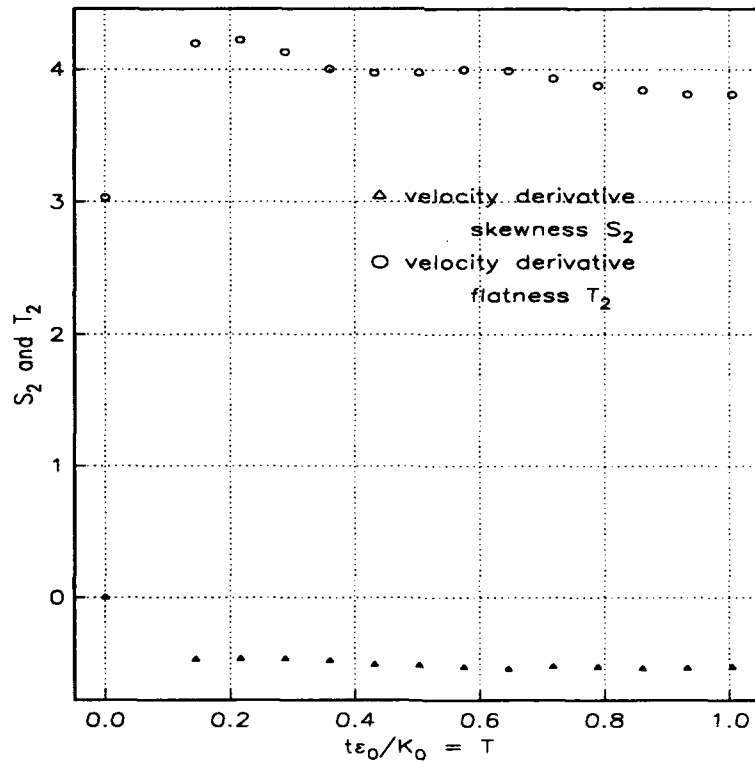


Figure 14: Velocity Derivative Skewness and Flatness.

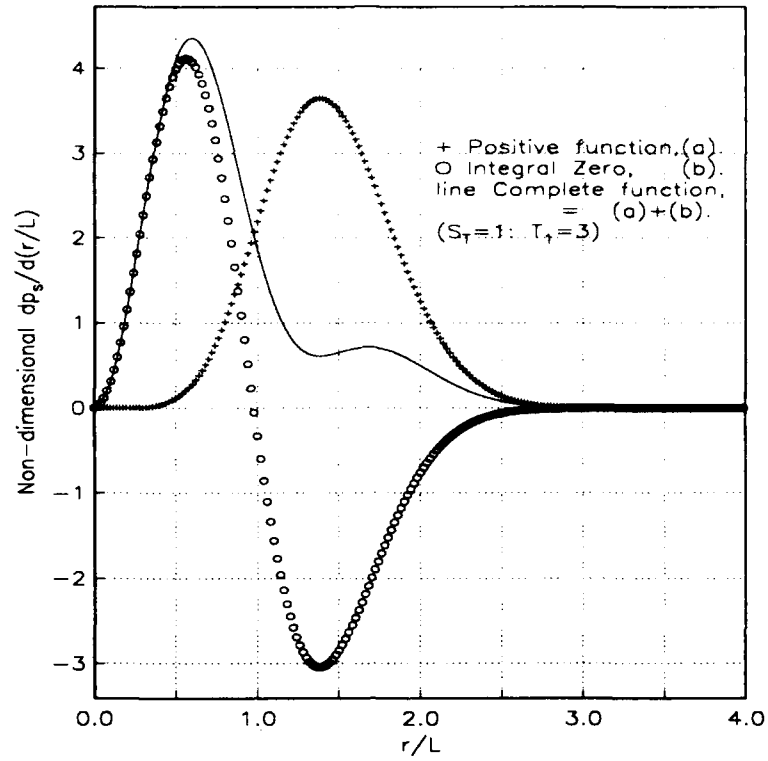


Figure 15: Acoustic Power Distribution Function.

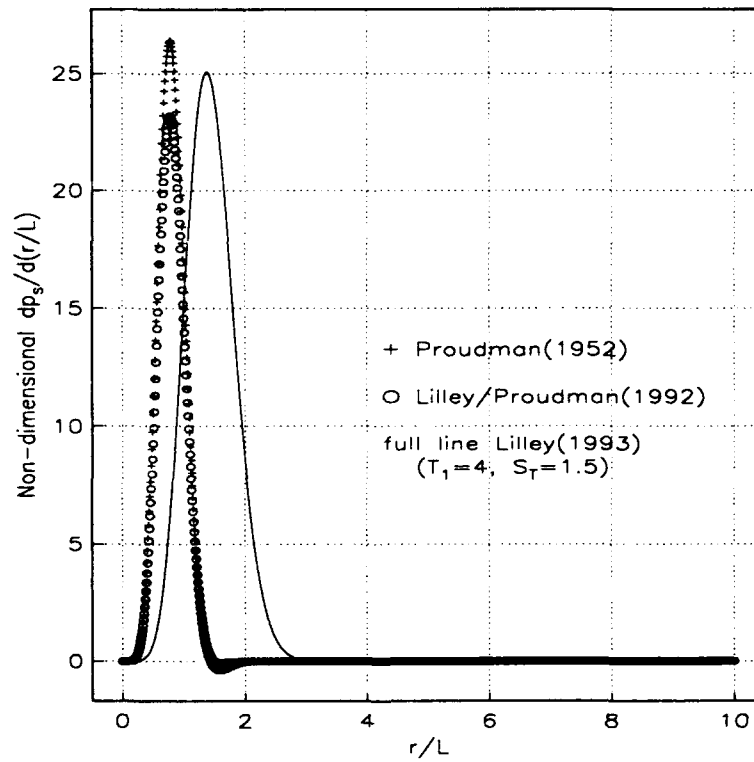


Figure 16: Acoustic Power Distribution Function.

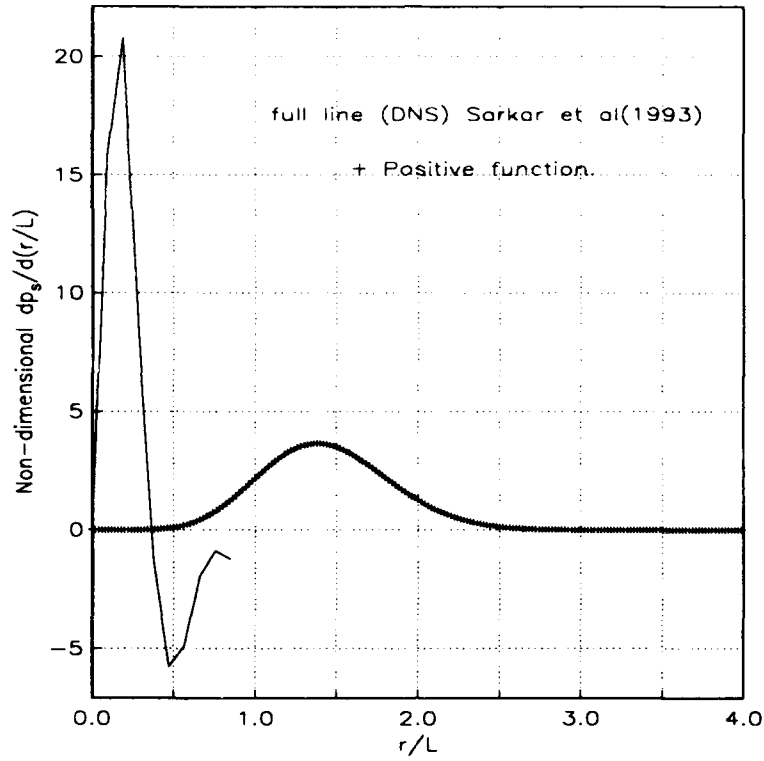


Figure 17: Acoustic Power Distribution Function.

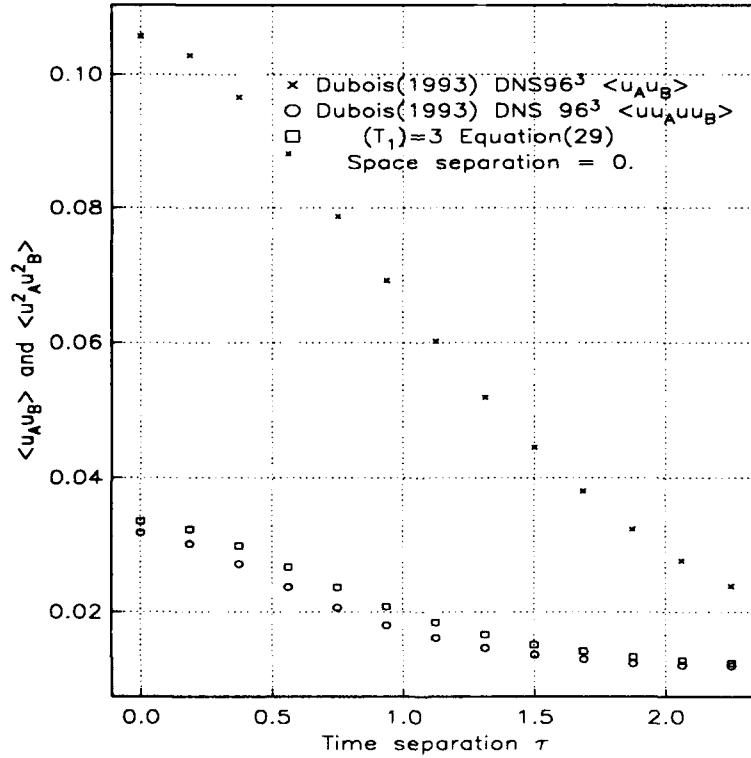


Figure 18: Comparison of Measured and Predicted $\langle u_A^2 u_B^2 \rangle$.

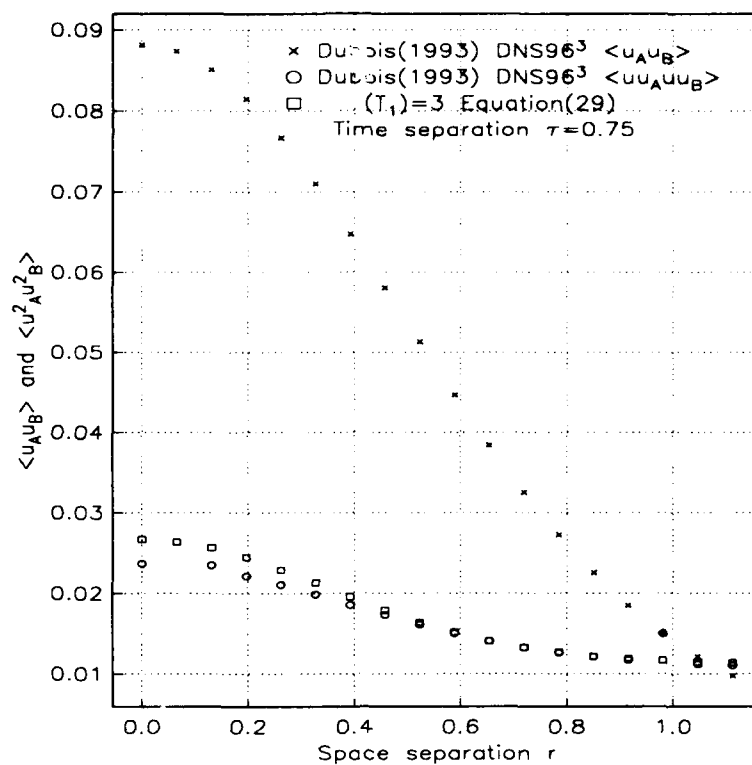


Figure 19: Comparison of Measured and Predicted $\langle u_A^2 u_B^2 \rangle$.

REPORT DOCUMENTATION PAGE			Form Approved OMB No 0704-0188	
Public reporting burden for this collection of information is estimated to average 1 hour per response, including the time for reviewing instructions, searching existing data sources, gathering and maintaining the data needed, and completing and reviewing the collection of information. Send comments regarding this burden estimate or any other aspect of this collection of information, including suggestions for reducing this burden, to Washington Headquarters Services, Directorate for Information Operations and Reports, 1215 Jefferson Davis Highway, Suite 1204, Arlington, VA 22202-4302, and to the Office of Management and Budget, Paperwork Reduction Project (0704-0188), Washington, DC 20503				
1. AGENCY USE ONLY(Leave blank)		2. REPORT DATE December 1993		3. REPORT TYPE AND DATES COVERED Contractor Report
4. TITLE AND SUBTITLE THE RADIATED NOISE FROM ISOTROPIC TURBULENCE REVISITED			5. FUNDING NUMBERS C NAS1-19480 WU 505-90-52-01	
6. AUTHOR(S) Geoffrey M. Lilley				
7. PERFORMING ORGANIZATION NAME(S) AND ADDRESS(ES) Institute for Computer Applications in Science and Engineering Mail Stop 132C, NASA Langley Research Center Hampton, VA 23681-0001			8. PERFORMING ORGANIZATION REPORT NUMBER ICASE Report No. 93-75	
9. SPONSORING/MONITORING AGENCY NAME(S) AND ADDRESS(ES) National Aeronautics and Space Administration Langley Research Center Hampton, VA 23681-0001			10. SPONSORING/MONITORING AGENCY REPORT NUMBER NASA CR-191547 ICASE Report No. 93-75	
11. SUPPLEMENTARY NOTES Langley Technical Monitor: Michael F Card Final Report Submitted to Theoretical and Computational Fluid Dynamics				
12a. DISTRIBUTION/AVAILABILITY STATEMENT Unclassified-Unlimited Subject Category 34			12b. DISTRIBUTION CODE	
13. ABSTRACT (Maximum 200 words) The noise radiated from isotropic turbulence at low Mach numbers and high Reynolds numbers, as derived by Proudman (1952), was the first application of Lighthill's <i>Theory of Aerodynamic Noise</i> to a complete flow field. The theory presented by Proudman involves the assumption of the neglect of retarded time differences and so replaces the second-order retarded-time and space covariance of Lighthill's stress tensor, T_{ij} , and in particular its second time derivative, by the equivalent simultaneous covariance. This assumption is a valid approximation in the derivation of the $\partial^2 T_{ij} / \partial t^2$ covariance at low Mach numbers, but is not justified when that covariance is reduced to the sum of products of the time derivatives of equivalent second-order velocity covariances as required when Gaussian statistics are assumed. The present paper removes these assumptions and finds that although the changes in the analysis are substantial, the change in the numerical result for the total acoustic power is small. The present paper also considers an alternative analysis which does not neglect retarded times. It makes use of the Lighthill relationship, whereby the fourth-order T_{ij} retarded-time covariance is evaluated from the square of similar second-order covariance, which is assumed known. In this derivation no statistical assumptions are involved. This result, using distributions for the second-order space-time velocity squared covariance based on the Direct Numerical Simulation(DNS) results of both Sarkar and Hussaini(1993) and Dubois(1993), is compared with the re-evaluation of Proudman's original model. These results are then compared with the sound power derived from a phenomenological model based on simple approximations to the retarded-time/space covariance of T_{xx} . Finally the recent numerical solutions of Sarkar and Hussaini(1993) for the acoustic power are compared with the results obtained from the analytic solutions.				
14. SUBJECT TERMS turbulence; acoustics; noise; sound			15. NUMBER OF PAGES 56	
			16. PRICE CODE A04	
17. SECURITY CLASSIFICATION OF REPORT Unclassified	18. SECURITY CLASSIFICATION OF THIS PAGE Unclassified	19. SECURITY CLASSIFICATION OF ABSTRACT	20. LIMITATION OF ABSTRACT	